Hindawi
Advances in Civil Engineering
Volume 2023, Article ID 7431292, 27 pages
https://doi.org/10.1155/2023/7431292

Research Article

Backcalculation of Finite-Element Modeling Based on Field Measurements Results of Excavation in Steel Sheet Pile Walls

Zoa Ambassa,[1,2] **Jean Chills Amba**,[1,2] **Merlin Bodol Momha**,[1] **and Landry Djopkop Kouanang**[1,2]

[1]*Laboratory of Energy Modeling Materials and Methods (E3M), National Higher Polytechnic School of Douala, University of Douala, P.O. Box 2701, Douala, Cameroon*
[2]*Department of Civil Engineering, National Higher Polytechnic School of Douala, University of Douala, Douala, Cameroon*

Correspondence should be addressed to Zoa Ambassa; zoaambassadaniel@gmail.com

Received 2 September 2023; Revised 30 October 2023; Accepted 27 November 2023; Published 21 December 2023

Academic Editor: Pengjiao Jia

The study presents a development of a nonlinear finite element calculation technique for the prediction of the stability of the multistaged deep excavation in submerged multilayered soft soil retained by steel sheet pile walls structures performed from Cast3M FE code. Optimization numerical backcalculation results are given for the design and construction of retaining walls with adjustment parameters, horizontal displacements, and earth and hydraulic pressure measurements. The difficulties of modeling 2D sheet pile walls in 2D with irregular shapes were overcome by transforming the geometry and stiffness of these sheet steel sheet pile walls into retaining walls of equivalent bending stiffness on the one hand and regular geometric shapes on the other hand. The results of this approach are satisfactory in view of the horizontal displacement curves obtained on the steel sheet pile walls compared by the measures.

1. Introduction

For decades, even after the development of robust numerical methods, stability analyses of retained walls are still carried out using traditional limit equilibrium approaches. The finite element technique represents a good approach for retained wall analysis which is accurate, versatile, and requires fewer a priori assumptions, especially, regarding the failure mechanism. Elastoplastic analysis of geotechnical problems using the finite element technique has been widely accepted in the research arena for many years; however, its routine use in geotechnical works for retaining stability analysis still remains limited. With finite element practice, we do not need to know the shape of the failure surface for stability calculations for example. Some engineers working in specialized design offices are often worried about the need to resort to such complexity, taking into account the poor quality of the data from soil properties often available from conventional field studies [1–3]. Although their concerns are often justified, there are certain types of geotechnical problems for which the numerical approach seems unavoidable. In this practice, the experienced engineer is challenged to know which type of problem requires the use of a numerical method and which is not. Structures with a predominance of nonlinear behavior such as the determination of settlements in soft soils and strains, the calculation of flow quantities due to stationary infiltration or the study of transient effects due to consolidation are all very likely to be solved by numerical methods. For regular geometry problems, the old traditional techniques using diagrams, tables, or graphical methods are adequate for regular geometry problems, but the numerical method approach seems necessary when irregular geometries or spatial variations of materials are encountered that cannot be handled by the old graphical solutions.

In common geotechnical practice, the use of a nonlinear method is justified by the fact that these calculations make it possible to see the area of failure of structures, despite a significant increase in complexity that may require the help of an expert in modeling [4]. Nonlinear treatments are always iterative because the problem data itself is a function of the "solution." However, concerns about these nonlinear

analyses that require excessive energy and time consumption have been largely outweighed by the performance of the computers and their reduced costs. The submerged soft soil retained by steel sheet pile walls is an area of geotechnical investigation structures using a nonlinear FE technique to have enormous advantages in contrast to traditional methods. As this study will show, retained wall analysis under multistaged deep excavation on soft soils by elastoplastic finite elements is fair, powerful, and relatively simple for application by professional engineers based on their experience.

The objective of this work is the development of an elastoplastic calculation method for the prediction of the stability of the multistaged deep excavation in submerged multilayered soft soil retained by steel sheet pile walls structures by finite element technique thanks to methodological and sophisticated computing from Cast3M FE code. Optimization numerical backcalculation results are proposed for retained steel sheet pile walls calculation and layout work based on the horizontal displacements measurements. The paper describes several standards in geotechnical practice of finite element retained wall analysis with comparison against field test measurements. In this context, this article improves the numerical modeling of layout work stages and hydromechanical coupling. The innovation of the study is focused on the following aspects: (1) the adoption of the simple geometric shape of the steel sheet pile walls whose bending stiffness is equivalent to the real geometric shape which does not allow 2D numerical modeling to be carried out without simplifying the geometry; (2) the use of the Cast3M FE code making it possible to compute the process of evolution of the calculations from the choice of finite element type of the model until the output phase; (3) the description of the soft soils on an advanced elastoplastic behavioral law of the Drucker–Prager type making it possible to realistically take into account the effects of nonlinearities in the materials; (4) modeling the excavation in staged construction as carried out on the site with taking into account the initial stresses and automatic recording of the results of the phase in the table; and (5) the verification of stresses, strains, and displacements at any point of the model according to functional requirements of such geotechnical work. Graphical outputs are included to illustrate displacements, strains, pressures, and failure mechanisms.

2. Literature Review of Finite Elements Analysis for Retaining Walls Stability

The considerable development of various cities around the world requires new techniques for occupying usable space to build infrastructure. Underground work is taking off considerably in order to provide users with frequent and regular means of transport. This work is not without danger, it can cause significant settlement and cracks on structures that are nearby [5–12]. The backfill behaviors on soft soils depend on the geotechnical parameters of the materials, the saturated or unsaturated state, the flow of the water table, the geometry, the environmental conditions, and the different stages of construction. The environmental stresses of structures and the soil around a retaining structure change over time, especially with fluctuations in the water table, and soil resistance decreases. Improper design of the excavation support structure can lead to serious engineering accidents and cause significant economic losses [13–15]. Therefore, it is necessary to take measures to considerably reduce the ground movements resulting from excavation and to control the parameters that guarantee proper operation under conditions of unquestionable safety, taking into account the interaction between the different parts of the geotechnical structure [4, 16]. The lateral displacement of the multilayer soft soil retained by steel sheet pile walls is highly dependent on the changing behavior of the materials depending on the variability of water retention, the geometry of the structure, and spatiotemporal considerations. Many theories have been proposed in literature to limit deformation and deflection on excavation supports by adjusting the design data to take into account the stepwise excavation [4, 16, 17]. A design method that allows oblique bending to be taken into account has been tested by Kort [18]. Based on the evaluation of the results of the large-scale field tests, his conclusion shows that the structure's response was consistent with the same expectations that were retained in the design basis for such works. The analysis of the interactions between the retaining walls structure, the grounds and the neighboring structures requires to improve the techniques of numerical simulation, notably the finite element method applied to retaining structures [19]. In this arena, Lim et al. [20] developed a spaceless earth excavation support in soft clay, called a rigid fixed membrane wall retaining system. It is composed of many structures: diaphragm walls, ribbed walls, transverse walls, and buttresses, as well as a complementary structure, the cap slab. The performance and mechanisms of this system have been studied by 3D finite element analyses by its promoter [20]. The results show that as the rigidity of the rigid fixed membrane system increases, the deformations induced by excavation decrease.

The angle effect was found in numerical analysis and the horizontal strains of the support structure were affected by the length of the excavation in a parametric study conducted on the stability of several excavation cases [6]. Considerations of several sets of parameters have shown that control indicators such as lateral deflections of the ground at the position of the bottom layer, vertical displacement of the soil surface, and vertical bearing load have clear spatial distribution characteristics. Several excavations with irregular geometries and spatial variability of materials have been studied and carried out in recent years, with major environmental stresses [16]. The prestressed earth retention (IPS) technique was proposed to be used in case the construction space is narrow. Several excavations have been carried out using this technique for its unique strengths, which gives it the ability to provide a larger workspace in tensioning the cables in order to limit the deformations of the wall with unquestionable safety guarantees [16]. The spatiotemporal consideration, allowing control of the strains caused by the shear resistance of the soil, which allows for minimal deformation of the retaining wall, measurements of layered soils, and plugged excavation were taken for reference [16]. The

analysis of the stability of the slopes and retained walls through the EF method has made it possible to obtain satisfactory results, making it essential in cases of irregular geometries. The finite element technique has also been used in a practical case of stability in the open-pit mining drifts of Yallourn, Victoria, Australia, allowing to validate of stability indicators in such workings. In order to really exploit the results of the measurements, the random fields were conditionally simulated using the finite element technique as part of a reliability analysis study of excavations in unsaturated soils with variable parameters from one zone to another [21]. The uncertainties resulting from the soil–structure interaction were taken into account by this method, by setting up a treatment of sufficiently smooth and sufficiently rough interior faces reducing to maximum and minimum values that can justify the entire range of possible solutions [21]. A probabilistic approach to the analysis of the digging method was carried out by the authors with and without consideration of suction in order to evaluate the influence of the unsaturated state on the braced support system. Gholampour and Johari [21] demonstrated in their results that the application of the unsaturated nature not only leads to changes in the statistical data of the structure's performance indicators but also to changes in the performance indicators of the structure, the position of the significant values. The use of FEM with reduction of resistance parameters including the effects of unsaturated transient infiltration and other primary numerical results concerning the stability of an earthen dam subjected to rapid drainage was carried out by Huang and Jia [22]. A stability analysis performed on the Yashigou earth dam in China was conducted by Huy et al. [23]. Ambassa et al. [17] conducted a finite element analysis of a soft soil reinforced by an industrial nailing technique using a soft soil behavior model. He determined the main influential parameters. Yang et al. [24] developed a method using a numerical model for the analysis of the stability parameter by determining of 3D fracture surfaces involved in a 3D analysis of slope safety. An enhanced strength reduction (ISRT) technique to avoid the appearance of uncontrolled area of large irreversible deformations in the bottom of a slope has been highlighted in the 3D numerical parameter variability technique, and an improved resistance reduction based on 3DNNM has been developed. Wong [25] has made a useful synthesis of the potential sources of error in the treatment of an EF modeling problem of the stability of slopes and retaining structures. Other important contributions in this area come from the work of Sloan [26] who published the paper concerning the progress of stability analysis combining the limit theorems of classical plasticity with finite elements to obtain rigorous maximum and minimum bounds concerning the breaking load. Its new development in finite element limit analysis incorporates pore water pressures and proposes new methods for obtaining stability solutions, including anchors, slopes, excavations, tunnels, and foundations. Tschuchnigg et al. [27] carried out a comparative study concerning the strength reduction technique and rigorous limit analyses that are based on the high deformation failure theorems.

The safety parameters for the stability of the different collapse forms taking into account the spatial variability of ground geotechnical parameters of the actual site in the unsaturated state were analyzed by Johari and Kalantari [28]. They studied the stochastic framework using a random elastoplastic finite element program coded in MATLAB. To obtain the design parameters of the system by composing the design parameters of the different collapse forms in the next step, Johari and Kalantari [28] used the sequential compounding technique. Regardless of the mode of failure, the numerical results showed that taking into account the condition of the ground-free soil increases the mean value of the safety parameter and decreases the associated standard deviation, which can be considered as an objective of the performance study. Lateral displacement is the most predominant component reliability index [28]. Johari and Peiro [29] made a stochastic study of a landslide on the side of a very busy road in an Asian country. Initially, they used aerial photographs, followed by measurements of the site and photographs showing a recently collapsed landslide. This information was supplemented in the field by geolocated soil samples used to obtain the geotechnical parameters necessary to feed realistic models of the behavior of these soils [29]. The stochastic back analysis approach was adopted because of the variability of these parameters across different sampling points. The optimized soil shear strength parameters were then calculated using the FEM program coded in MATLAB [29]. The results showed a more computationally efficient back analysis approach. The improvement of the consideration in an optimized way in stochastic analysis was conducted in order to obtain shear strength parameters allowing a better elucidation of the slope failure mechanism and become a fundamental indicator for more effective filtering of field remedial data [29]. Bozkurt et al. [30] performed finite element calculations involving the reconstituted materials to study the behavior of a deep excavation supported by sheet pile walls and columns composed of a mixture of two hydraulic binders. Huge displacements associated with installation methods have been observed despite the fact that the application of this lime–cement deep mixing technique in deep excavations improves soil parameters in its natural state [30]. In the study, the behavior of the structure composed of soil stabilized by two hydraulic binders was studied using the finite element technique by progressive disbursement of the soil layers. The data and modeling parameters were calibrated according to the results of actual measurements carried out at the site [30]. The lessons learned in these modeling show that taking into account the installation mode in the calculations makes it possible to predict in a realistic and optimized way the strains on the sheet pile walls, the evolution of the excess pore pressure, as well as the structural forces in the struts [30].

The developments which follow in this paper are inspired by these important contributions on this topic.

3. Methodology

After this literature review related to the problem, the methodology adopted in this study consists first of all in

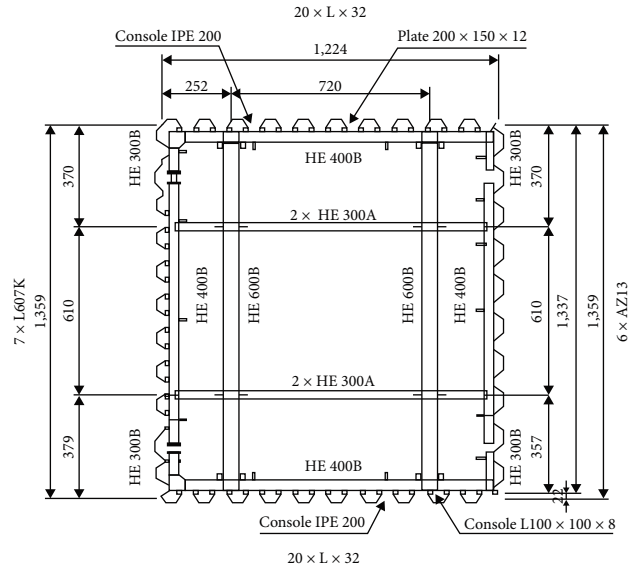

Figure 1: Strutting plan of sheet wall field test [18].

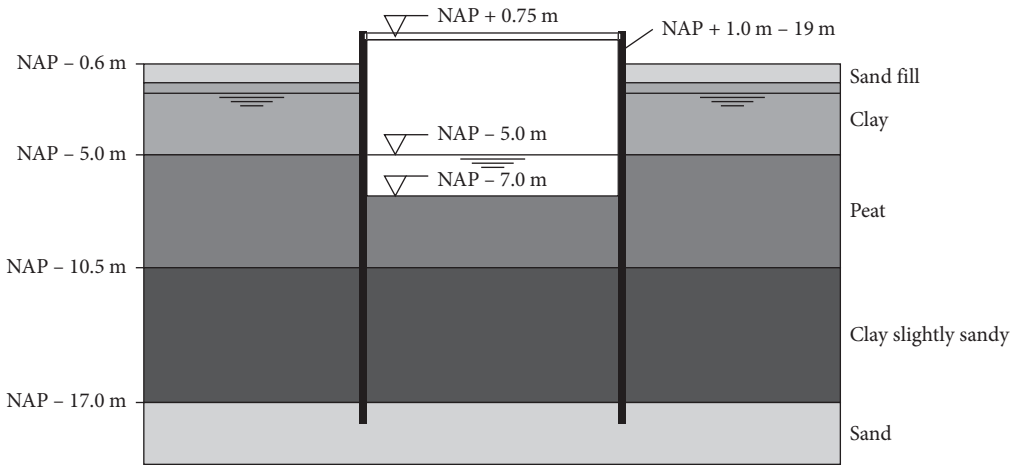

Figure 2: Sideview of sheet wall field test [18].

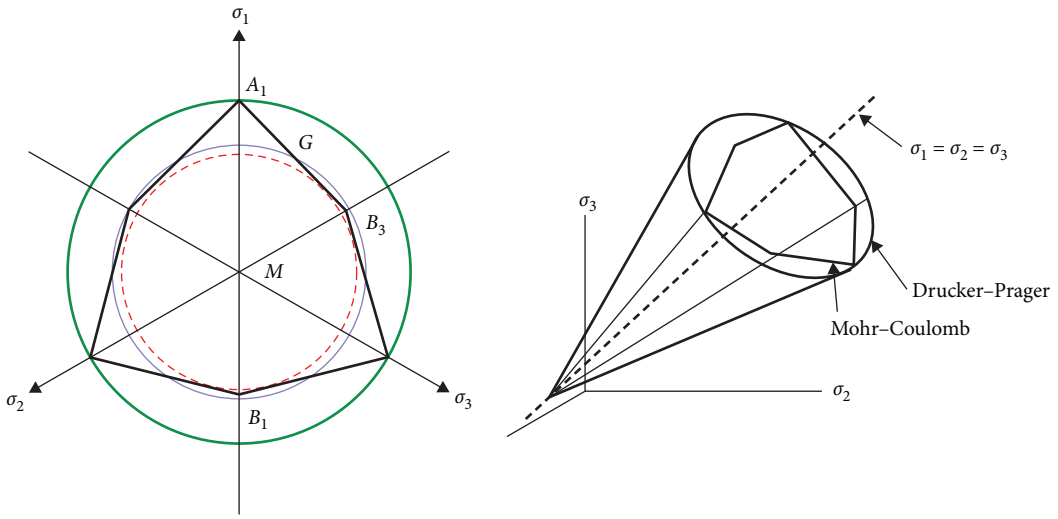

Figure 3: Mohr–Coulomb and Drucker–Prager yield criteria.

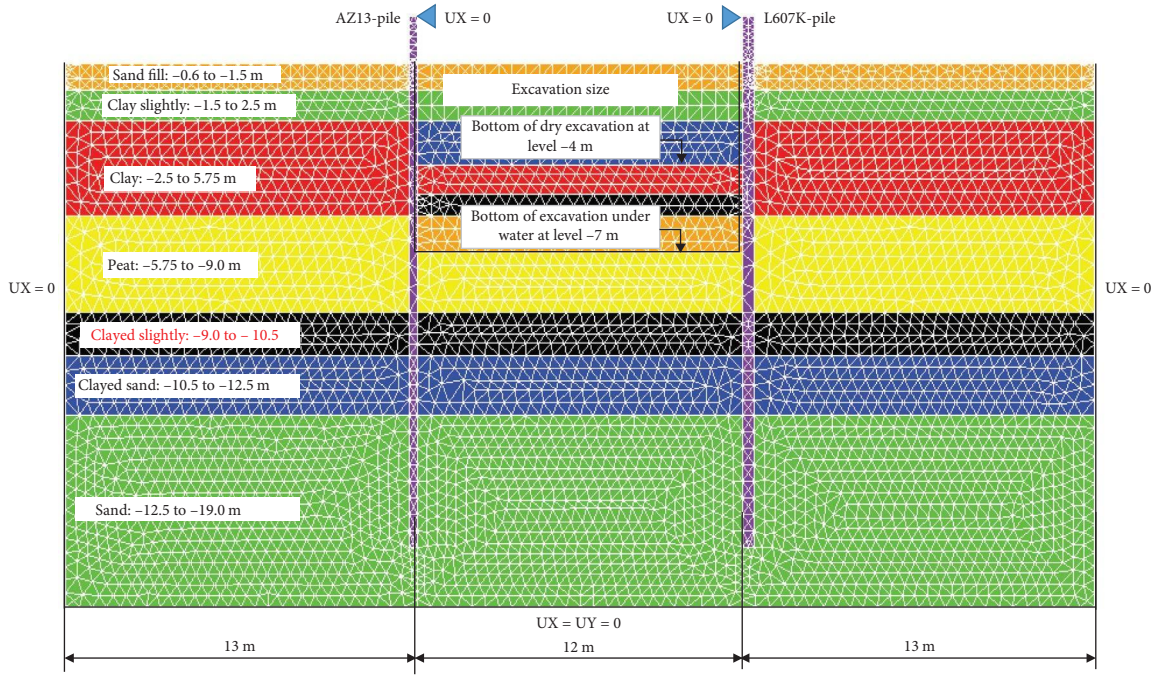

Figure 4: Detailed view of the 2D mesh and soil clusters of the deep excavation in submerged multilayered soft soils retained by two steel sheet pile walls.

Table 1: Structural properties of the AZ13-pile and the L607K-pile.

Pile	A (cm^2/m)	I (cm^4/m)	W (cm^3/m)	EI$_{yy}$ (kNm^2/m)	M (kg/m^2)	b (cm)	h (cm)	t_f (mm)	c (mm)
AZ13	137	19,700	1,300	41,370	107	67	30.3	9.5	–
L607K	244	70,030	3,220	147,260	192	60	43.5	–	146

Note. A = sheet pile area per metre; I = sheet pile inertia per metre; W = sheet pile inertia modulus per metre; EI = bending stiffness per metre; M = mass per square metre; b = sheet pile width; and h = sheet pile right-of-way height.

describing the site location of the geotechnical structures design aspects.

3.1. Layout of the Test Site. The test site was situated near Pernis, which is a suburb west of Rotterdam (Netherlands). In the Pernisserpark, a small area of land was available, about 20×50 m, where the field test could be carried out. Figures 1 and 2 display the layout of the sheet pile walls. The plan of the struts' walings is given in Figure 1. The horizontal displacement curves of the test wall were determined on the site from inclinometer measurements [18].

3.2. Behavior Laws of Soft Soil Materials. Numerical finite element modeling necessarily begins the characterization, on the one hand, the behavior of the soil ground constituting the structures whose stability is sought to be assessed by choosing an elastoplastic law to represent them, and on the other hand, in estimating in a relevant way a value deterministic for each of the parameters of the constitutive law, which associated with other variables, will constitute the input data of the finite element model. The choice of a realistic law depends on the mechanism to be modeled, the data available for the structures, but above all on the precision sought and numerical considerations. We are interested in the mechanisms that can lead structures under extreme stress to failure. However, to calculate the stability relating to the behavior of geotechnical structures by the FE technique, the assessment of the elastic strains does not matter because it is the modeling of the appearance and the increase of the unstabilized plastic strains which is important. Among the laws at our disposal and described in Mestat [31], we present here two classic behavior laws of the elastoplastic type: those of Mohr–Coulomb and Drucker–Prager. These two laws have the advantage of depending on a few parameters directly from triaxial and oedometric tests. They allow a certain "economy" of data acquisition and management which are, in particular those concerning the mechanical characterization of materials, relatively few in number and not very varied on geotechnical projects.

The Mohr–Coulomb criterion is the first that was proposed for soils [31]. It is used for long-term frictional and cohesive soils. It is characterized by the below relations:

$$F(\sigma ij) = (\sigma_1 - \sigma_3) - (\sigma_1 + \sigma_3)\sin\varphi - 2c\cos\varphi \leq 0, \quad (1)$$

$$G(\sigma_{ij}) = (\sigma_1 - \sigma_3) - (\sigma_1 + \sigma_3)\sin\psi + c^{\text{ste}}, \quad (2)$$

where c is the shear strength of the material in terms of vertical effective stress equal to zero, φ is the angle of

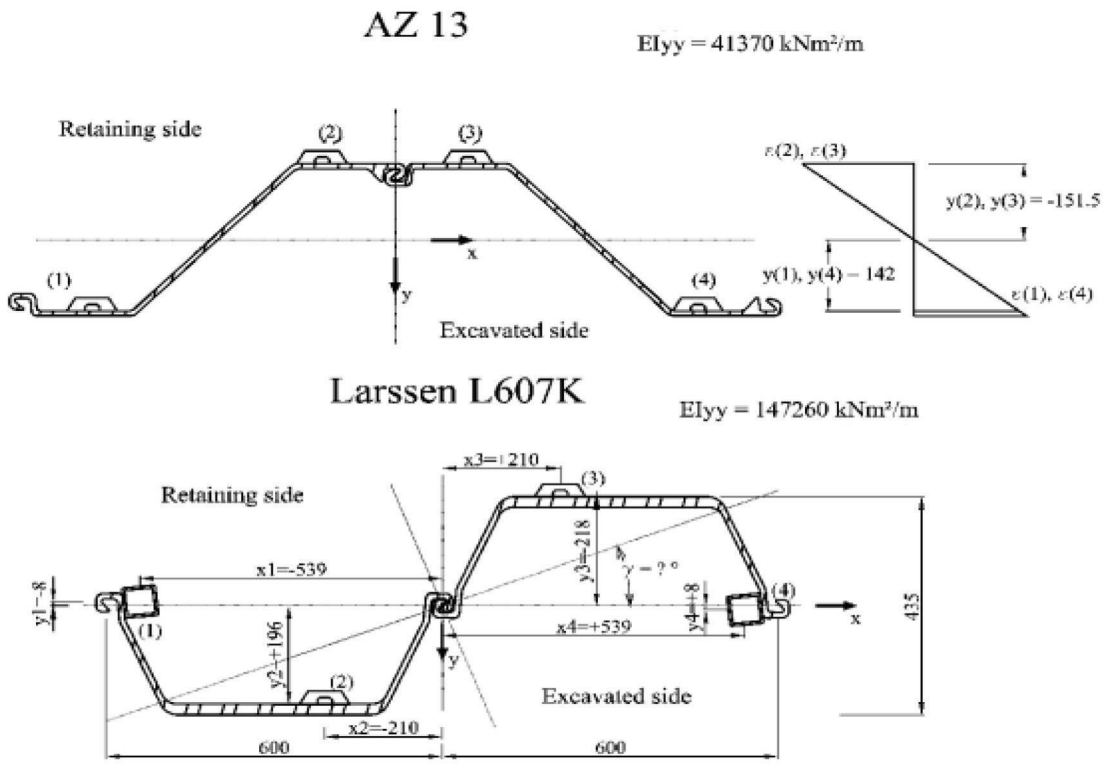

Figure 5: Dimensions of AZ13 and Larssen 607K position of strain gauges.

Table 2: Mechanical properties of the AZ13-pile and the L607K-pile used for numerical modeling.

Pile	I^{eq} (cm^4/m)	EI$_{yy}$ (kNm^2/m)	b (cm)	h (cm)	h^{eq} (cm)	E^{eq} (MPa)	Poisson ratio	γ (kN/m^3)	Type of model	Type of behavior
AZ13	225,000	41,370	67	30.3	30	18,467.3	0.2	24	Linear elastic	Nonporous
L607K	710,000	147,260	60	43.5	44	13,574.6	0.2	24	Linear elastic	Nonporous

shearing resistance, and ψ is the dilatancy angle. σ_1 and σ_3 represent the principal stresses ($\sigma_1 \geq \sigma_2 \geq \sigma_3$). In the principal stress space, the surface defined by the Mohr–Coulomb criterion is a hexagonal pyramid with an axis ($\sigma_1 = \sigma_2 = \sigma_3$) (Figure 3). Analogies are possible between the Mohr–Coulomb and Drucker–Prager criteria (Figure 3). Relations can be established between the parameters (α, γ, k) and (φ, ψ, c) in certain situations [31]. The Drucker–Prager criterion is written as follows:

$$f(\sigma) = \sqrt{J_2} + \alpha I_1 - K \leq 0, \tag{3}$$

$$f(\sigma) = \sigma_e + \sin \alpha I_1 - K' \leq 0. \tag{4}$$

The correspondence between the Mohr–Coulomb criteria and those of Drucker–Prager are as follows [32]:

$$\alpha = \eta = \frac{2\sqrt{3}\sin\varphi}{9 - \sin^2\varphi}, \gamma = \frac{2\sqrt{3}\sin\psi}{9 - \sin^2\psi}, K = \mathrm{KL} = \frac{6\sqrt{3}c.\cos\varphi}{9 - \sin^2\varphi}, \tag{5}$$

Moreover, the choice of a criterion must also be guided by the possible numerical difficulties of implementing the criterion. Some constitutive laws, such as that of Mohr–Coulomb for example, have a failure criterion comprising singular edges (Figure 3), which can numerically result in convergence difficulties [32–37]. In view of the above, the Drucker–Prager model implemented in the Cast3M finite element code will be used in this paper for the description of the elastoplastic behavior of soft soil materials.

4. Numerical Modeling

The numerical modeling of the deep excavation in submerged multilayered soft soil retained by steel sheet pile walls structures is made in 2D, plane strains from the finite

Table 3: Soft soil properties of the model.

Parameter	Symbol	Sand	Clayed sand	Clayed slightly	Peat	Clay	Sand fill	Unit
Material model	Model	Mohr–Coulomb	Mohr–Coulomb	Mohr–Coulomb	Mohr–Coulomb	Mohr–Coulomb	Mohr–Coulomb	–
Type of behavior	Type	Drained	Drained	Drained	Drained	Drained	Drained	–
Unit weight	γ'	10	6.34	3.9	2.3	6.75	17	kN/m^3
Permeability $\times 10^{-9}$	k_v	0.3	0.3	0.3	1.0	0.6	10,000	m/s
Young's modulus	E_{ref}	26×10^3	7.32×10^3	2.92×10^3	2.34×10^3	5.33×10^3	17.3×10^3	kN/m^2
Poisson's ratio	ν	0.3	0.2	0.2	0.2	0.2	0.3	–
Cohesion	c'	11.5	15.05	8.7	14.9	17.2	5.0	kN/m^2
Friction angle	ϕ'	38.3	16.83	16.7	18.37	18.15	35.0	Degree
Dilatancy angle	ψ	0	0	0	0	0	0	Degree

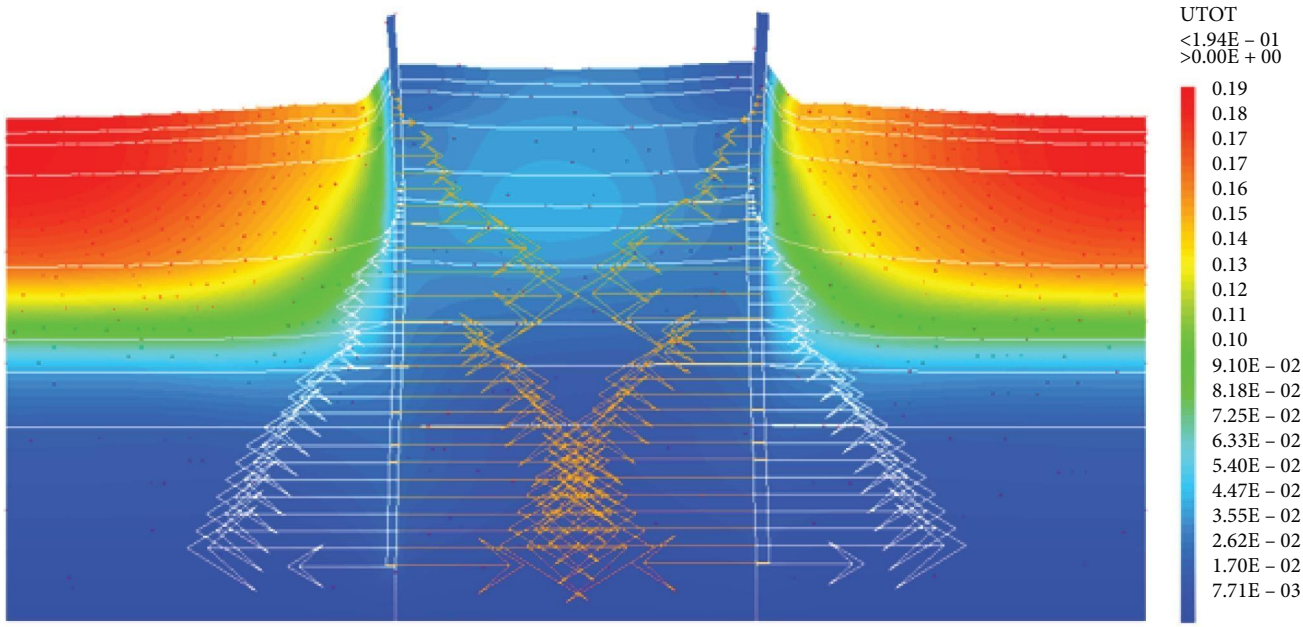

Figure 6: Shadings of the deformed of the total displacements: U (m) of the model.

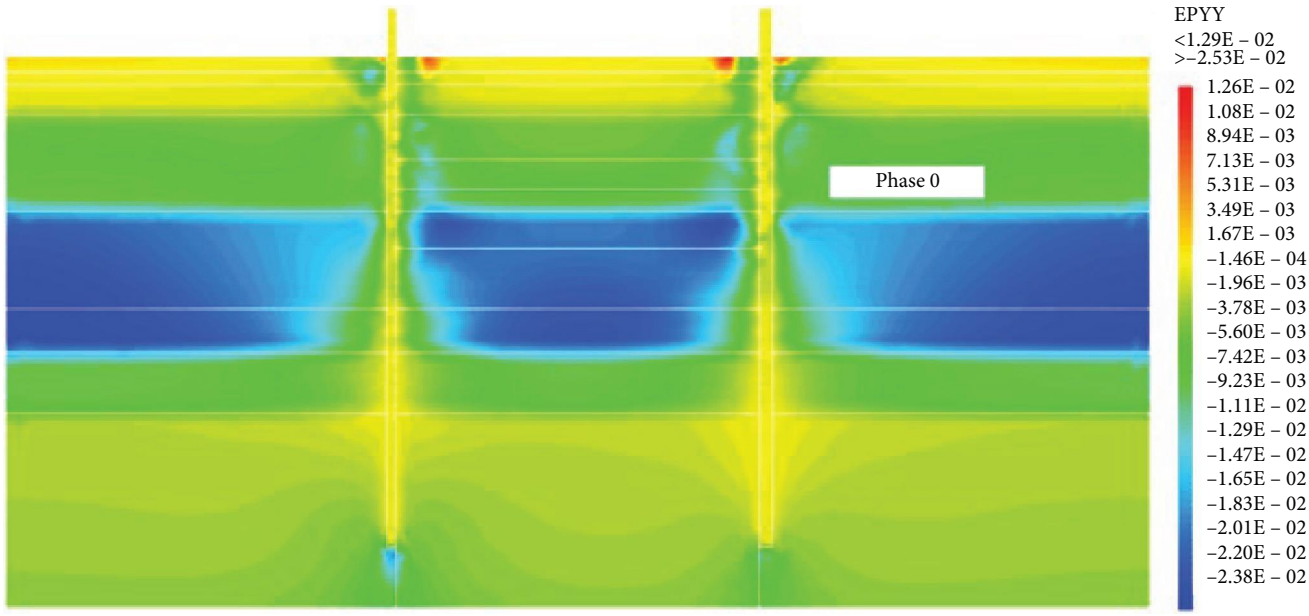

Figure 7: Shadings of the vertical strains of the model.

elements Cast3M [38] calculation code with triangular elements (7,910 elements) with six nodes (TRI6). The 2D mesh view of the numerical model and the borehole log with the altimetry of the different soils is displayed in Figure 4. The conditions for limiting the displacements at the ends of the model are classical, i.e., blocking of all displacements at the bottom of the model ($Ux = Uy = 0$) and blocking of horizontal displacements on the bound of the model ($Ux = 0$). Zero groundwater flow is also fixed on the steel sheet pile walls and the bottom, left, and right bound of the model. In this study, the load generated by the self-weight of the soil is computed using a standard gravity "turnon" procedure involving integrals over each element of the form:

$$p^{(e)} = \gamma \int_{V^e} N^T d(\text{vol}), \tag{6}$$

where N values are the shape functions of the element and the superscript e refers to the element number. This integral evaluates the area of each element, multiplied by the total unit weight of the soil, and distributes the net vertical load consistently to all the nodes [4, 39–42]. These element loads

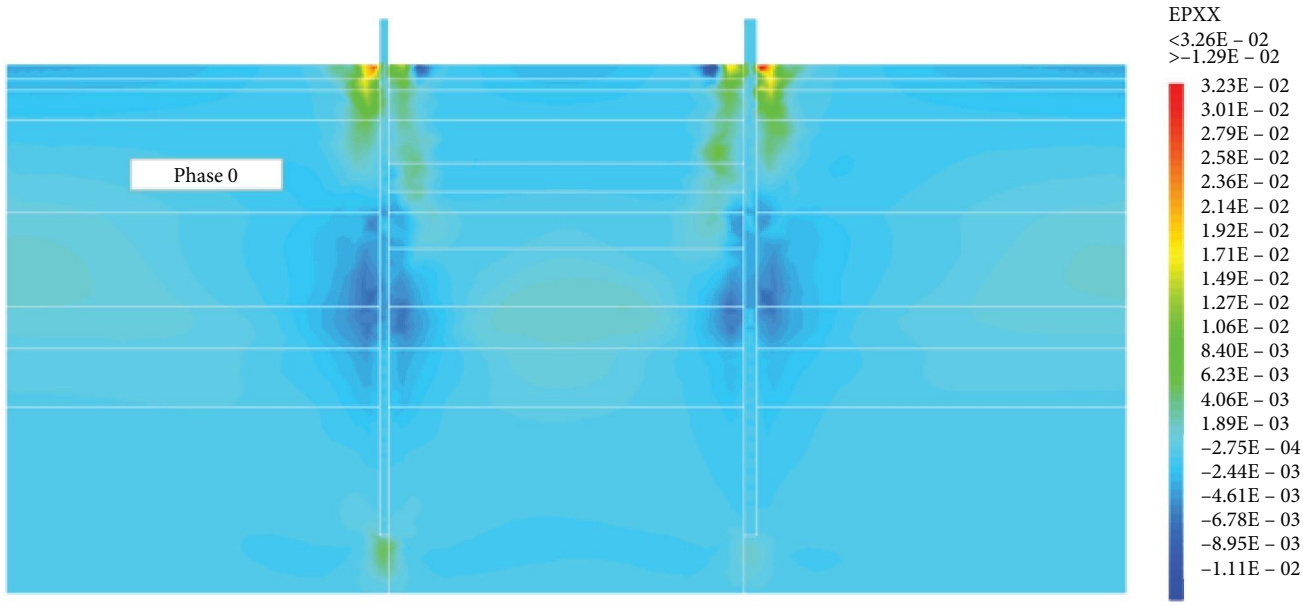

Figure 8: Shadings of the horizontal strains of the model.

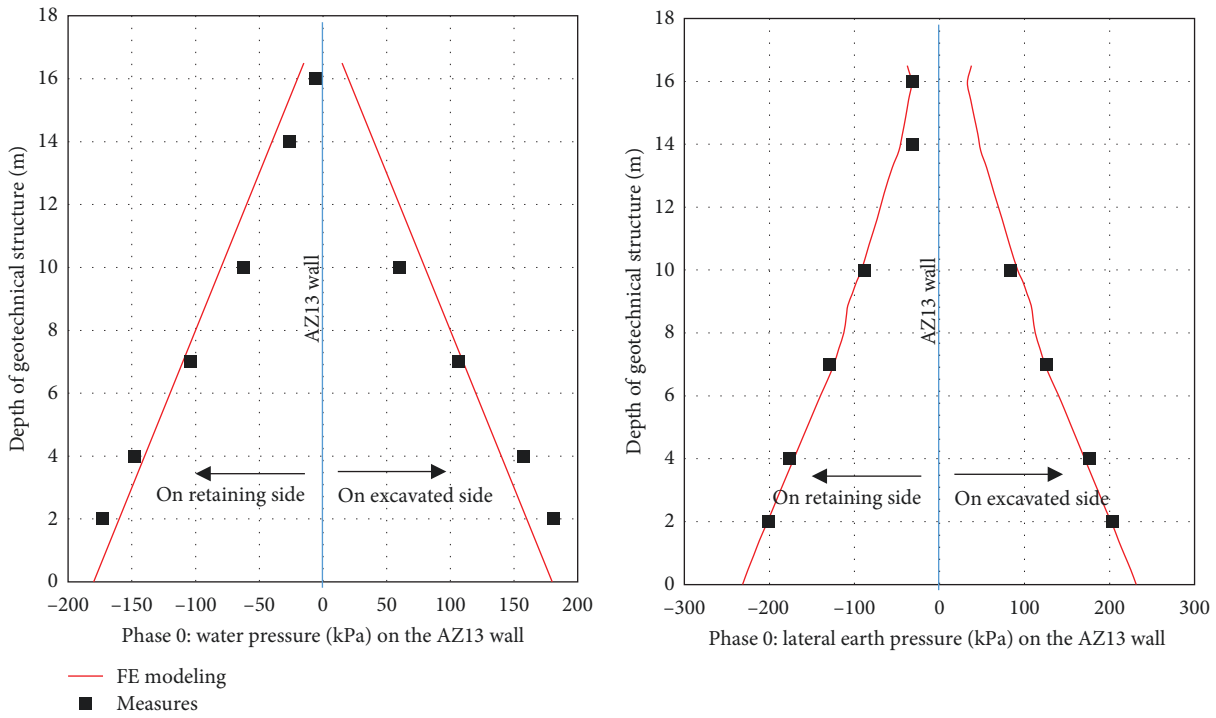

Figure 9: FE modeling vs. measurement results of the water pressure and the lateral earth pressure for the AZ13 wall.

are assembled into a global gravity force vector that is applied to the FE mesh in order to generate the initial stress state of the problem.

4.1. Materials Model. The properties of the AZ13 and the L607K steel sheet piles were presented (Table 1 and Figure 5), and the struts are made of metal beams of high inertia; they are therefore assumed to be infinitely stiff. The simulation of the struts supports was made by imposing a zero horizontal displacement for the two points of support (see Figure 4). Sheet pile walls are modeled by massive elements. The material is assumed to be isotropic linear elastic; Young E's modulus is calculated assuming the conservation of bending stiffness. The inertia of AZ13 sheet pile is evaluated at 19,700 cm^4/m, which leads to an inertia product equal to 41,370 kNm^2. The steel sheet piles AZ13 and L607K were modeled as retaining walls of uniform thickness $h = 30$ cm and $h = 44$ cm, respectively, of equivalent modulus of elasticity

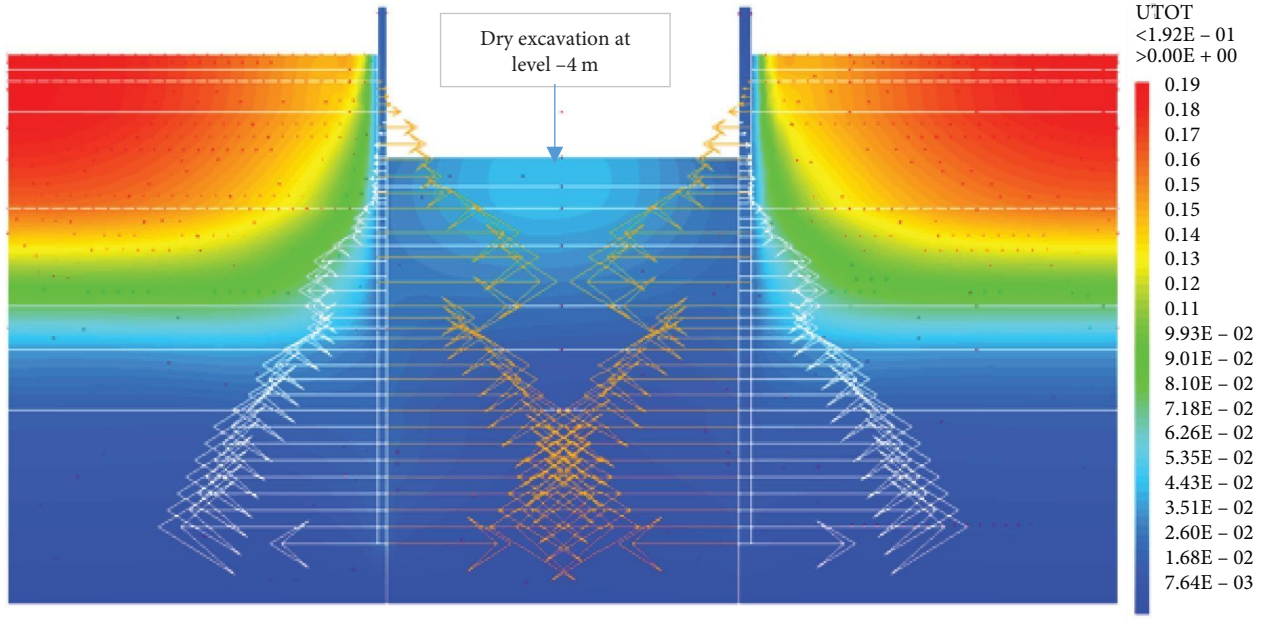

Figure 10: Shadings of the total displacements (m) of the model in phase 1.

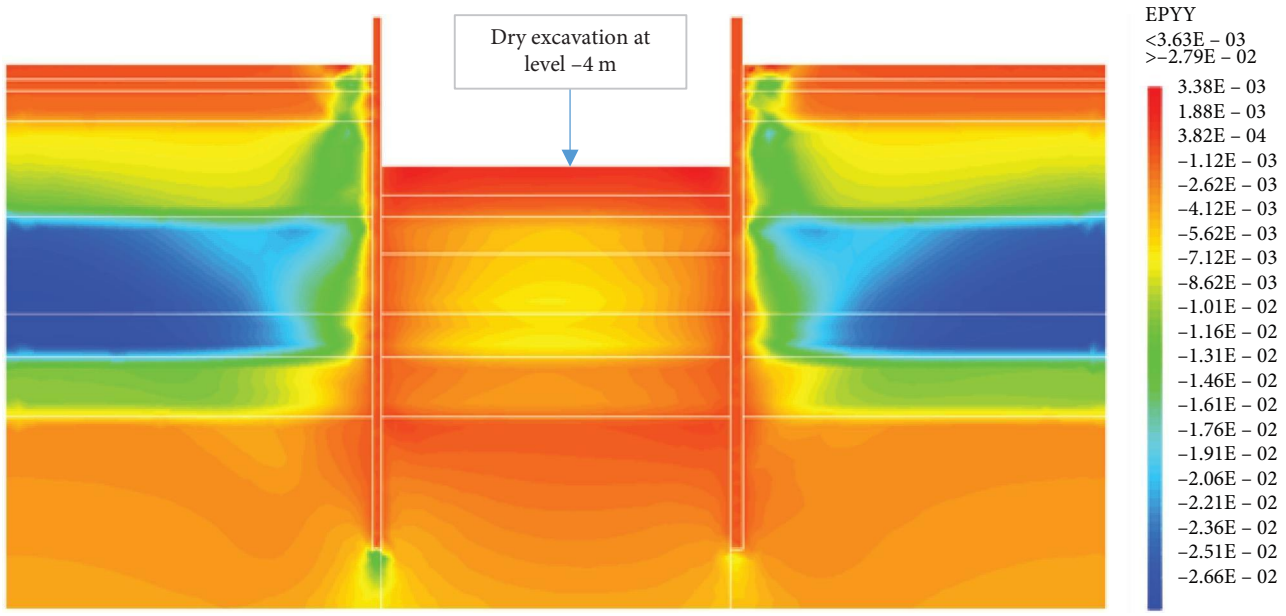

Figure 11: Shadings of the vertical plastic strains of the model in phase 1.

equal to $E^{eq}_{AZ13} = 18,467.3$ MPa and $E^{eq}_{L607K} = 13,574.6$ MPa. The equivalent modulus is given by $E^{eq} = \frac{EI}{I^{eq}}$ where I^{eq} is the equivalent inertia of the uniform wall section considered (Table 2). The soil data used in the calculations are those derived from the triaxial tests. The geotechnical parameters used were collected (see Table 3). Drucker–Prager model [43], ideal elastoplasticity without hardening or softening, the constant stiffness parameters are adjusted intrinsic parameters of the mean Mohr–Coulomb compression and tensile. Apart from the volume weight γ, the modulus of deformation E, and Poisson's ratio, this model requires eight additional parameters, some of which are deduced from the Mohr–Coulomb model for its use in the F.E Cast3M code. Its other parameters are as follows:

$$\alpha = \eta = \frac{2\sqrt{3}\sin\varphi}{9 - \sin^2\varphi}, \tag{7}$$

$$\alpha = \beta = \Delta = \sqrt{\frac{2}{3}}, \tag{8}$$

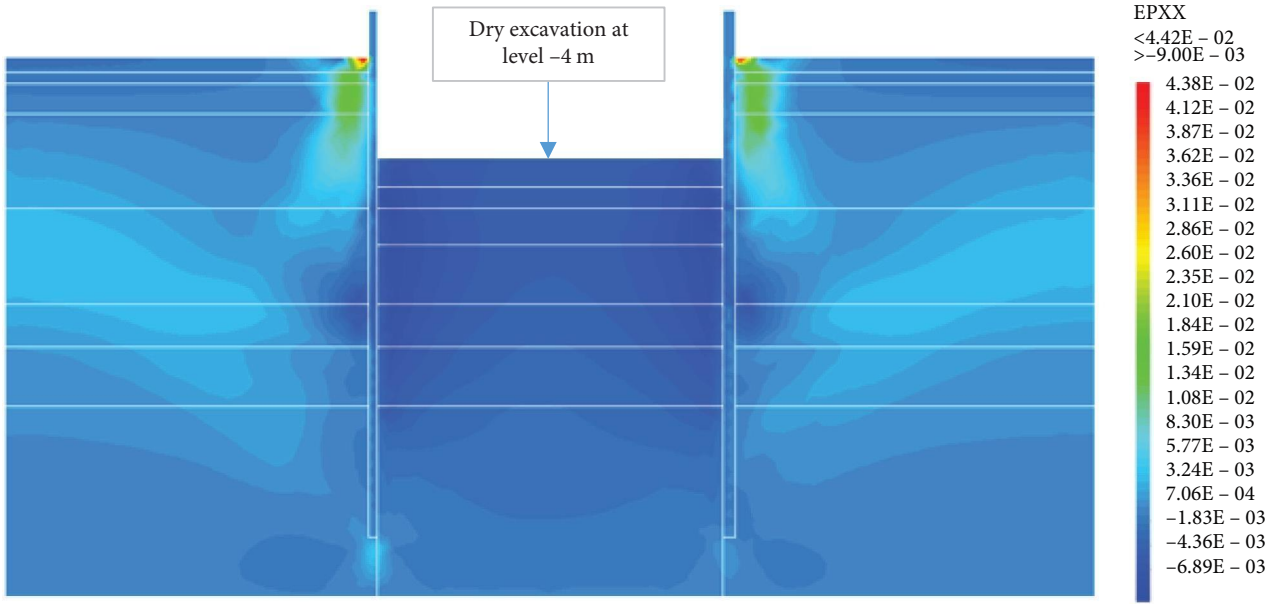

Figure 12: Shadings of the horizontal plastic strains of the model in phase 1.

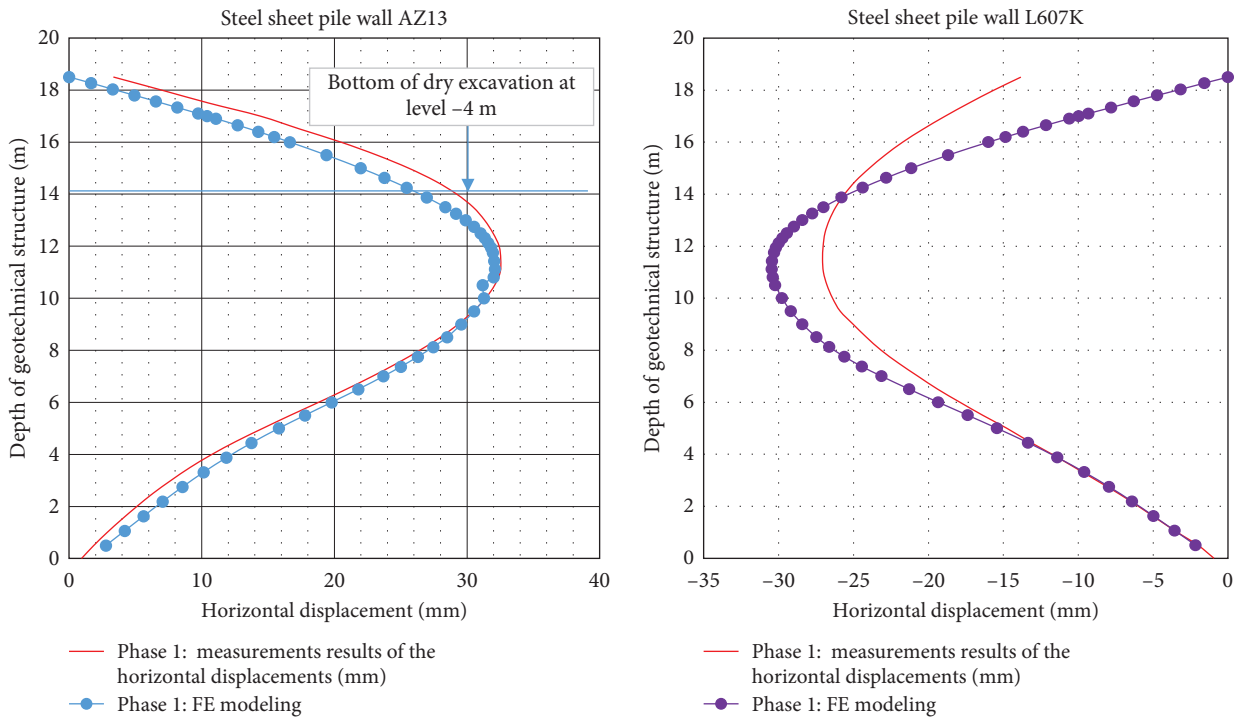

Figure 13: Horizontal displacements in the steel sheet pile walls in phase 1.

$$K = \mathrm{KL} = \frac{6\sqrt{3}c \cdot \cos\varphi}{9 - \sin^2\varphi}, \tag{9}$$

$$\gamma = \frac{2\sqrt{3}\sin\psi}{9 - \sin^2\psi}. \tag{10}$$

In our computations on Cast3M, we have used a variable FCYS (FaCtor Yield Surface) for the built-in Drucker–Prager plasticity model. For the Mohr–Coulomb strength parameters adjustment to the circular cone of the Drucker–Prager failure surface (see Figure 3), different strategies are known. The factor FCYS regulates the adjustment [44]. The value of 0.0 is tension, 1.0 is compression, and 0.5 is their average. Other values would mean a weighted result and values above 1.0 use the surface equality approach. Values below 0.0 default to 1.0 and the compression adjustment. In this paper, FCYS is fixed at 0.5. Table 3 presents the soil properties of the model.

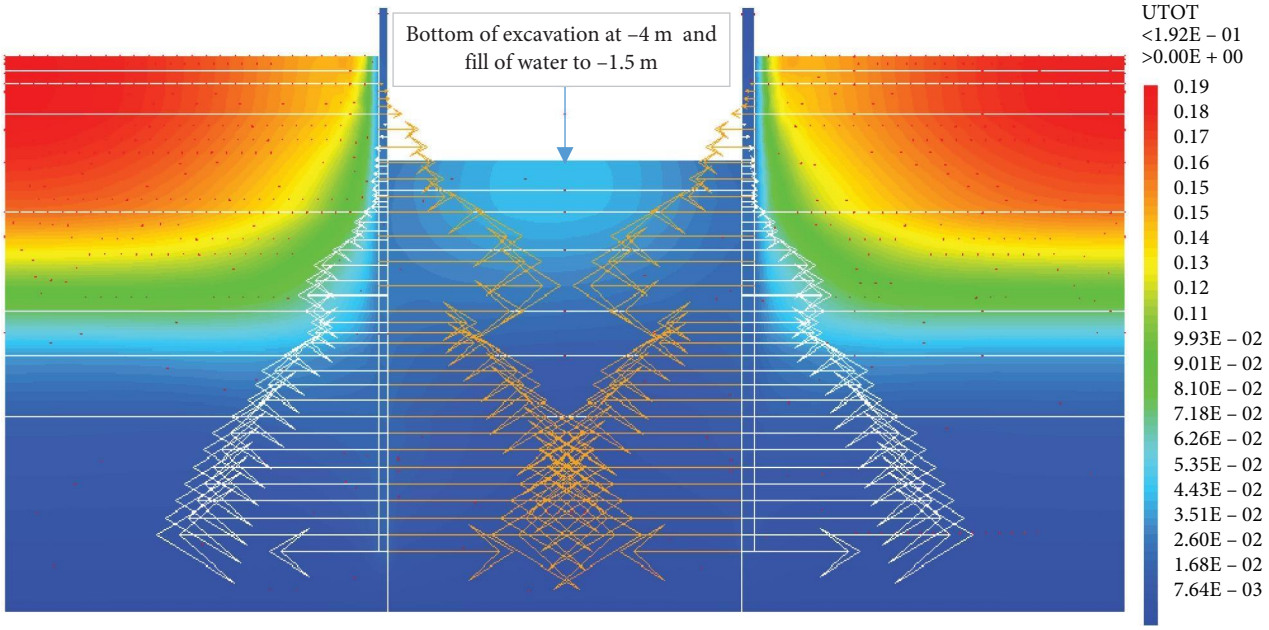

Figure 14: Shadings of the total displacements (m) of the model in phase 2.

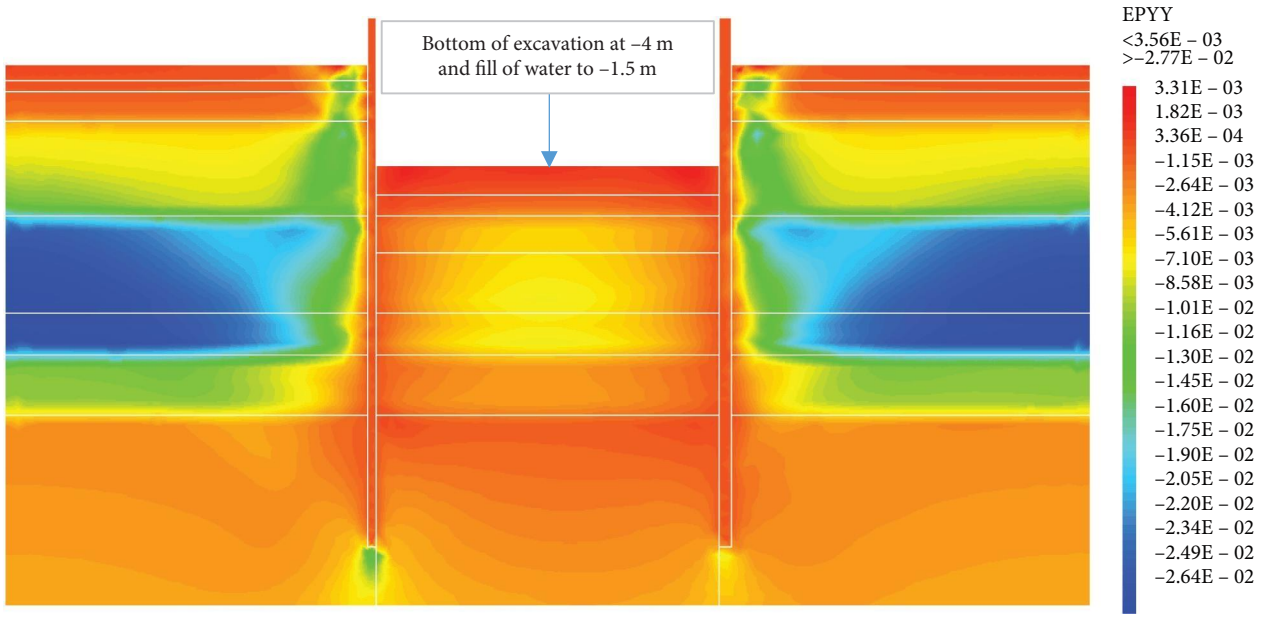

Figure 15: Shadings of the vertical plastic strains of the model in phase 2.

$\beta = \mu = \Delta = \sqrt{\frac{2}{3}}$ is implementation specific for Drucker–Prager model in Cast3M.

4.2. Modeling of the Excavation Procedure. To know the contribution of each phase depending on the functional requirements of the geotechnical structure, an elastoplastic calculation of stress–strain type is carried out and the displacements are calculated. The solution strategy is based by treatment of the problem in 2D plane strains (geometry and mesh), the definition of soils and retaining walls and the application of all self-weight and charges and the implementation of the excavation phases by progressive removal of the soil [45]. The following staged constructions are analyzed in Cast3M: phase 0 is based on the application of geostatic stress state in the sand fill from 0.65 to −1.5 m. In phase 1, the dry excavation to −4.0 m is realized. The fill with water is observed in phase 2 to −1.5 m. In phase 3, the excavation underwater to −7.0 m is realized. The lowering water level to −5.0 m is made in phase 4. The fill with water is observed in phase 5 to −1.5 m. The construction of sand backfill at left of AZ13 steel sheet pile is realized for phase 6. The falling water table to −5.0 m is made in phase 7 and the long-term performance is analyzed in phase 8.

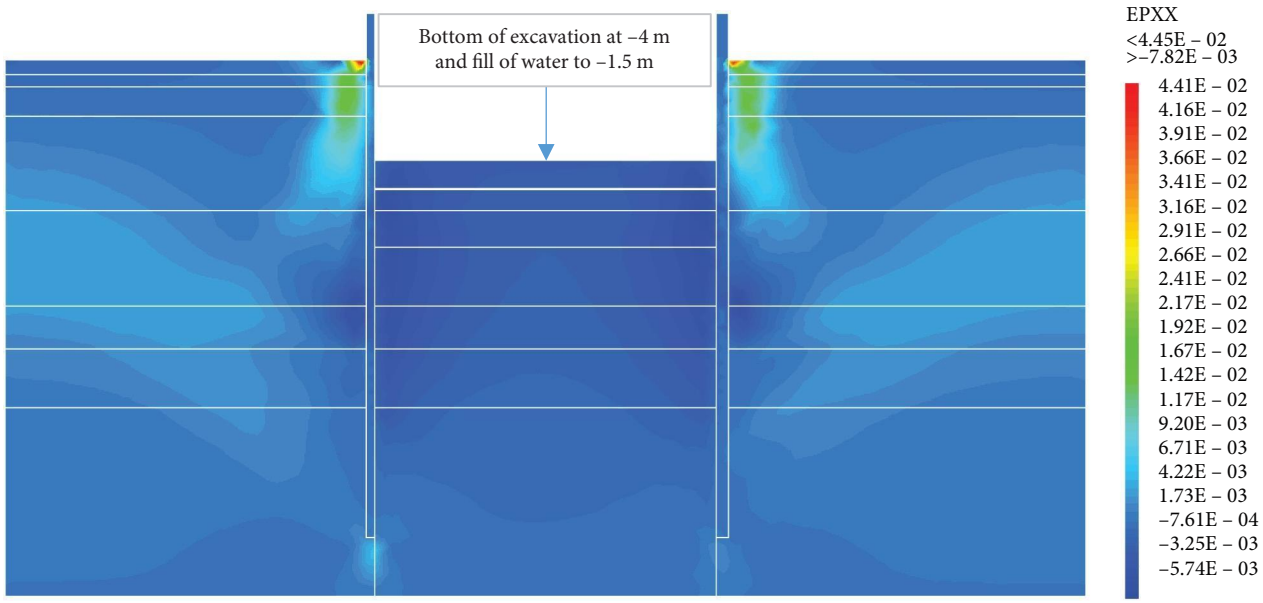

Figure 16: Shadings of the horizontal plastic strains of the model in phase 2.

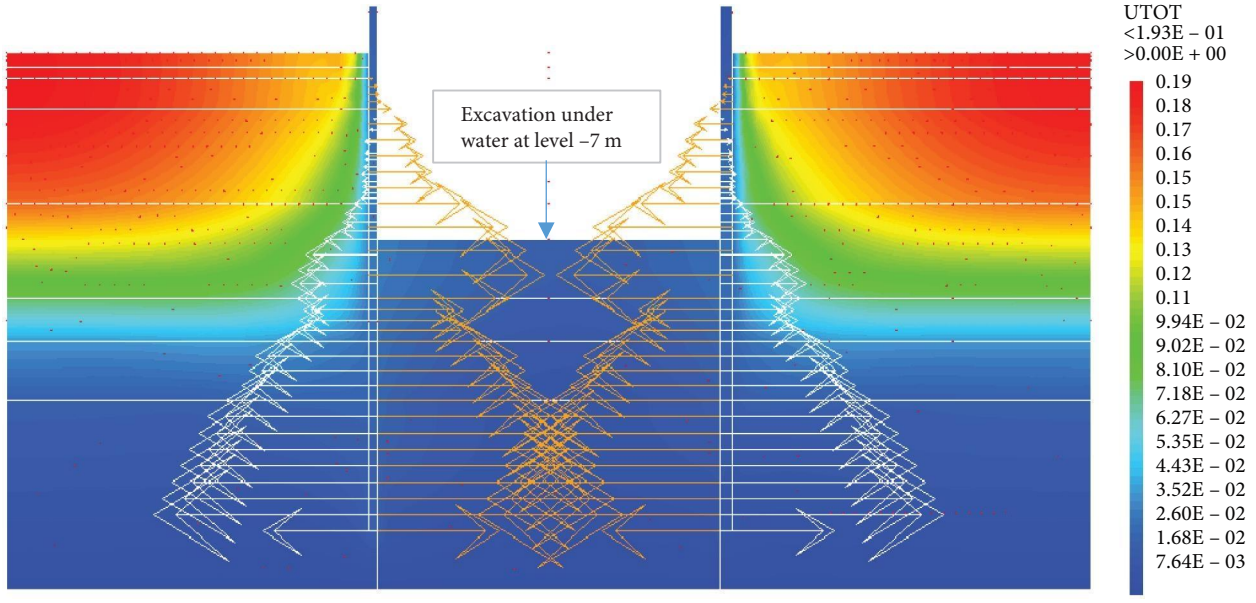

Figure 17: Shadings of the total displacements (m) of the model in phase 3.

5. Drucker–Prager Elastoplastic Modeling in Staged Excavation

In this part, the stresses and displacements are calculated for each excavation/construction stage. The "turn-on" procedure is described clearly according to the following calculation steps: after generation of the mesh of the global model, the calculation of the elastic phase is performed in order to obtain the stresses and the elastic displacements in the structure. The elastoplastic calculation is carried out in the code Cast3M on the basis of the initial stress calculated PASAPAS:

$$G_n = \| f - K(\varphi_k, c_k, \Psi_k, \sigma_t) u_n \| < \varepsilon, \tag{11}$$

where G represents the elastoplastic method, f represents the total force mobilized during the computation time in the model, K is the matrix of design plastic parameters as a function of angle of shearing resistance, dilatancy angle, and shear strength of the material in terms of vertical effective stress equal to zero, u_n is the displacement obtained during computation time n who depends of design parameters and the ultimate force mobilized, and ε represents the relative error of the method.

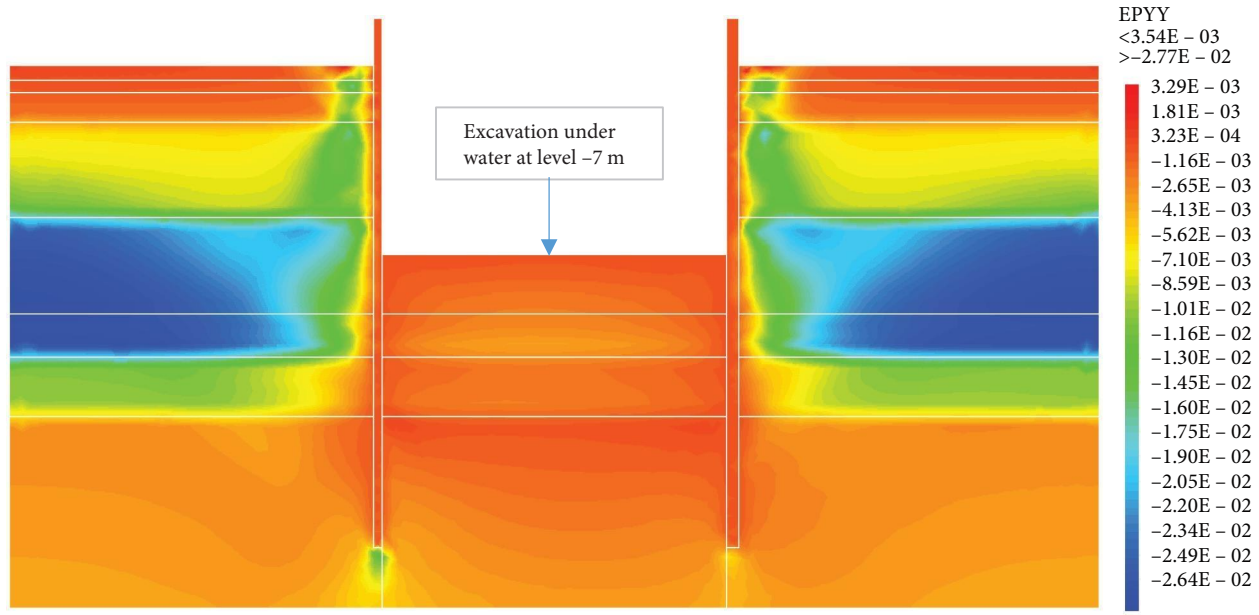

FIGURE 18: Shadings of the vertical plastic strains of the model in phase 3.

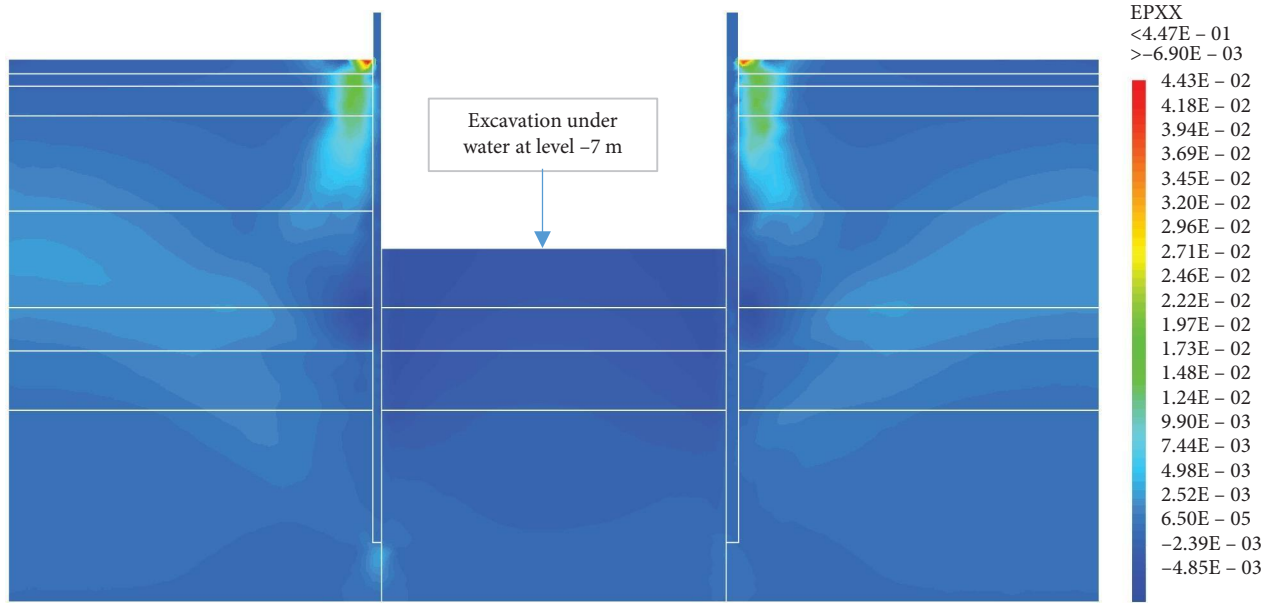

FIGURE 19: Shadings of the horizontal plastic strains of the model in phase 3.

The geostatic stress analysis is based on the existence of soil layers specified by the user during calculation. The vertical stress in the ith layer is calculated according to the following equation:

$$\sigma_i = \Sigma h_i \cdot \gamma_i. \tag{12}$$

In the case where the layer is below the water table, the unit weight of the layer below the water table is specified using the input data as follows:

$$\gamma_{su} = \gamma_{sat} - \gamma_w \quad \text{or } \gamma_{su} = (1 - n)(\gamma_s - \gamma_w), \tag{13}$$

where h_i is the thickness of the ith layer, γ_i is the unit weight of soil, γ_{sat} is the saturated unit weight of soil, γ_w is the water density weight, n is the porosity, and γ_s is the specific weight of soil.

Each excavation/construction stage of the structure corresponds to a PASAPAS calculation phase in the Cast3M code. In each phase, the parameters of the entire model are inserted and the calculation results are logged in a table. The phase number corresponds to the number of calculation tables.

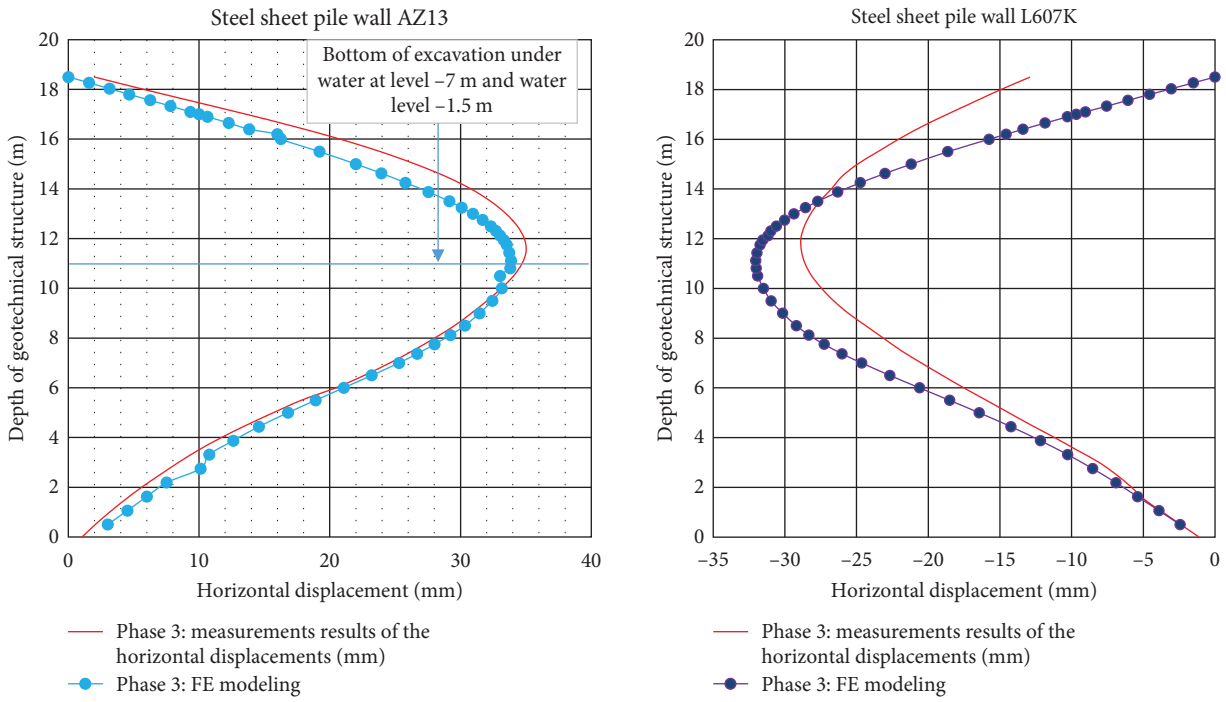

Figure 20: Horizontal displacement in the steel sheet pile walls in phase 3.

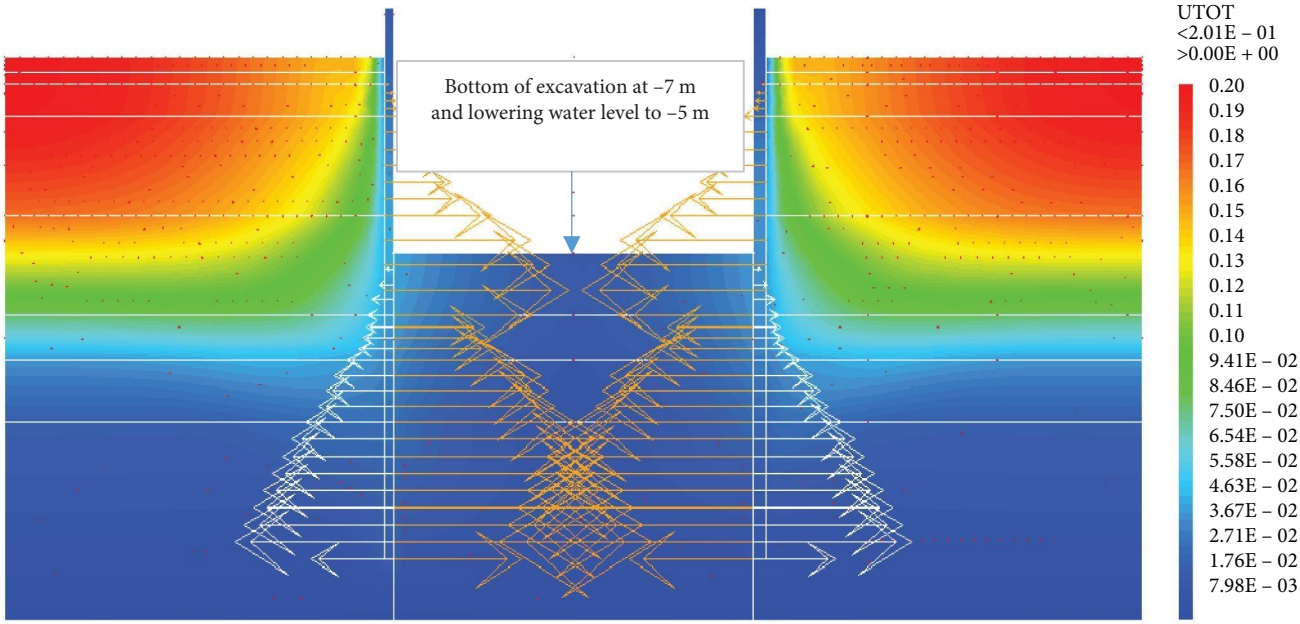

Figure 21: Shadings of the total displacements (m) of the model in phase 4.

5.1. Phase 0: Ground and Sand Fill. The purpose of the elastoplastic calculation carried out is to obtain the stresses and displacements throughout the model. The entire soil ground is built in a single phase. The gravity load is applied on the model. The importance of this phase is to assess the relevance of the modeling assumptions taken (walls, soil behavior, 2D plane strains, etc.). Figures 6–9 present the displacements, the strains, the water pressure, and lateral earth stress. The water and lateral earth stress obtained by FE modeling is compared by those from measurements [18, 19].

The total displacements are of the order of 19 cm on the surface of the sand backfill. This displacement clearly shows the behavior of the soft soil. This observation is confirmed by the shadings of the vertical plastic strains with a very high concentration in peat of the order of -2.53×10^{-3}. The validation of the FE modeling is done by comparing the results

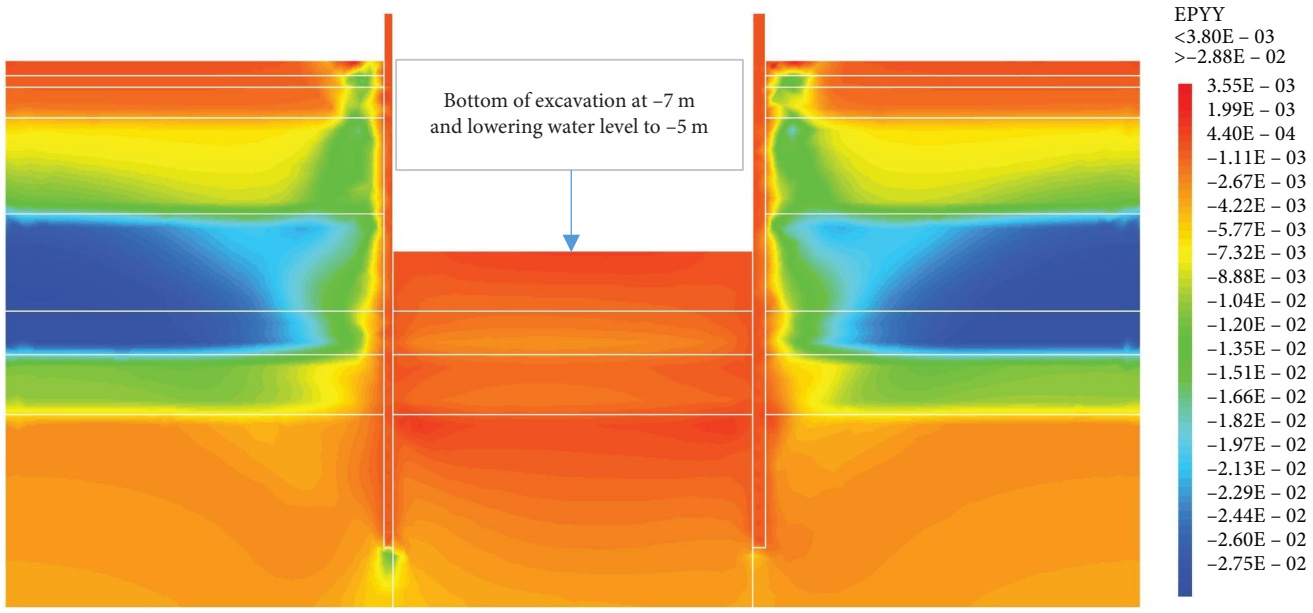

Figure 22: Shadings of the vertical plastic strains of the model in phase 4.

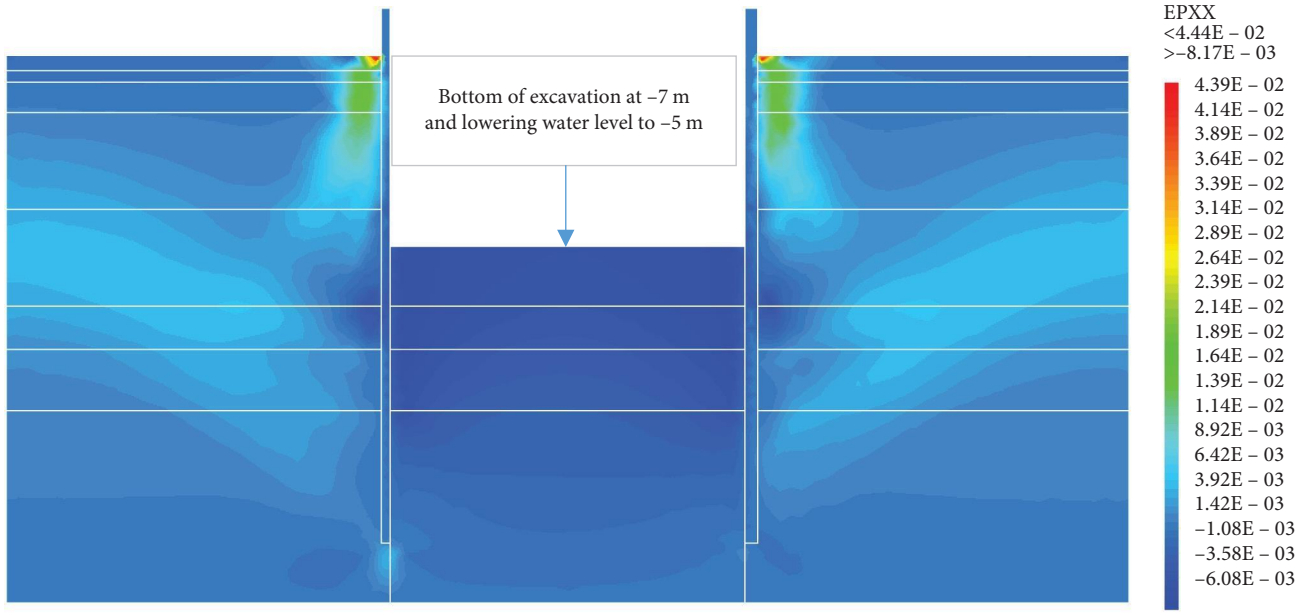

Figure 23: Shadings of the horizontal plastic strains of the model in phase 4.

of the model with those of on-site measurements. The results of hydraulic pressures and lateral earth pressures around the AZ13 wall are presented in Figure 9. A perfect concordance is observed (FE results vs. measurement results), thus validating the assumptions of the FE modeling taken.

5.2. Phase 1: Dry Excavation to −4.0 m. This phase is based on the dry excavation of geostatic stress state in the ground. The excavation of the soft soils between the two walls induces a total displacement of 19 cm out of the excavation and about 3.5 cm inside the excavation. Figures 10–12 present the total displacements, plastic strains, and vertical stress (phase 1) of the model from elastoplastic analysis. A perfect consistency is observed on the horizontal displacements within the excavated zone on the walls AZ13 and L607K (Figure 13). The difference between the results of calculations and measurements remains small.

5.3. Phase 2: Fill with Water to −1.5 m. Phase 2 is based on the fill with water from −4.0 to −1.5 m. In view of the results of this

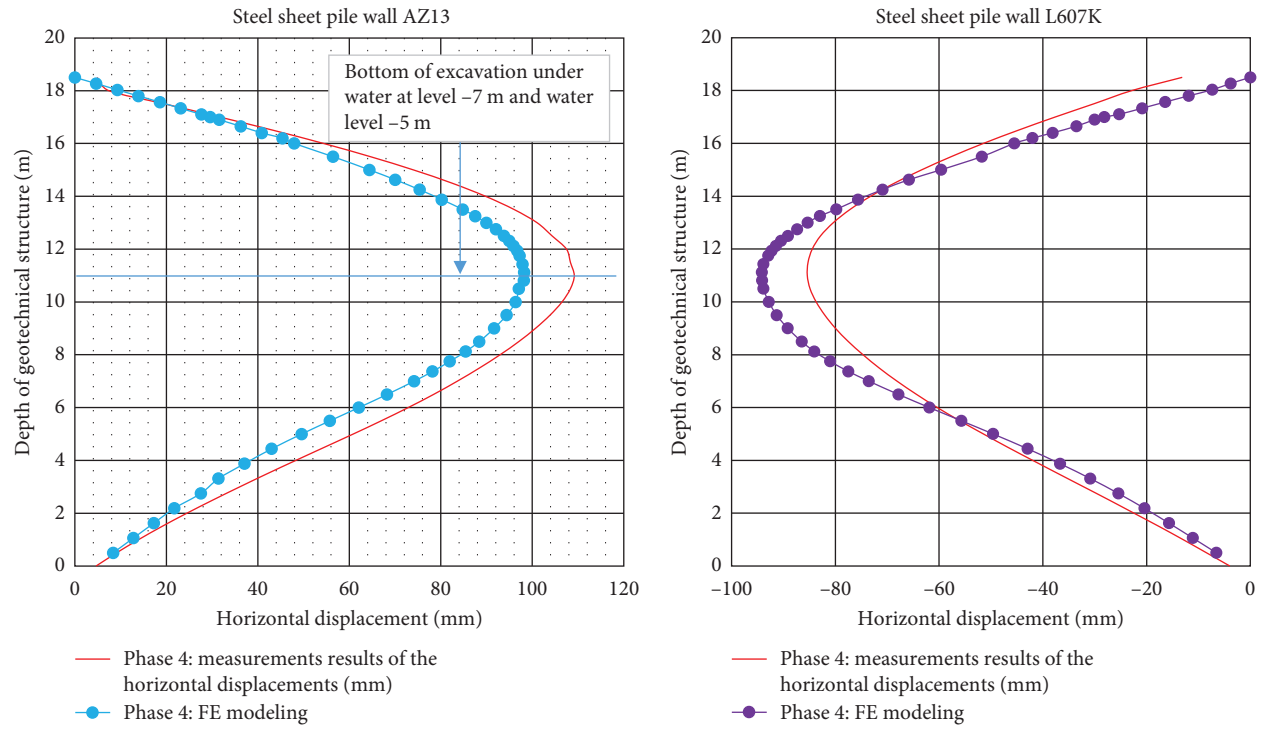

Figure 24: Horizontal displacement in the steel sheet pile walls in phase 4.

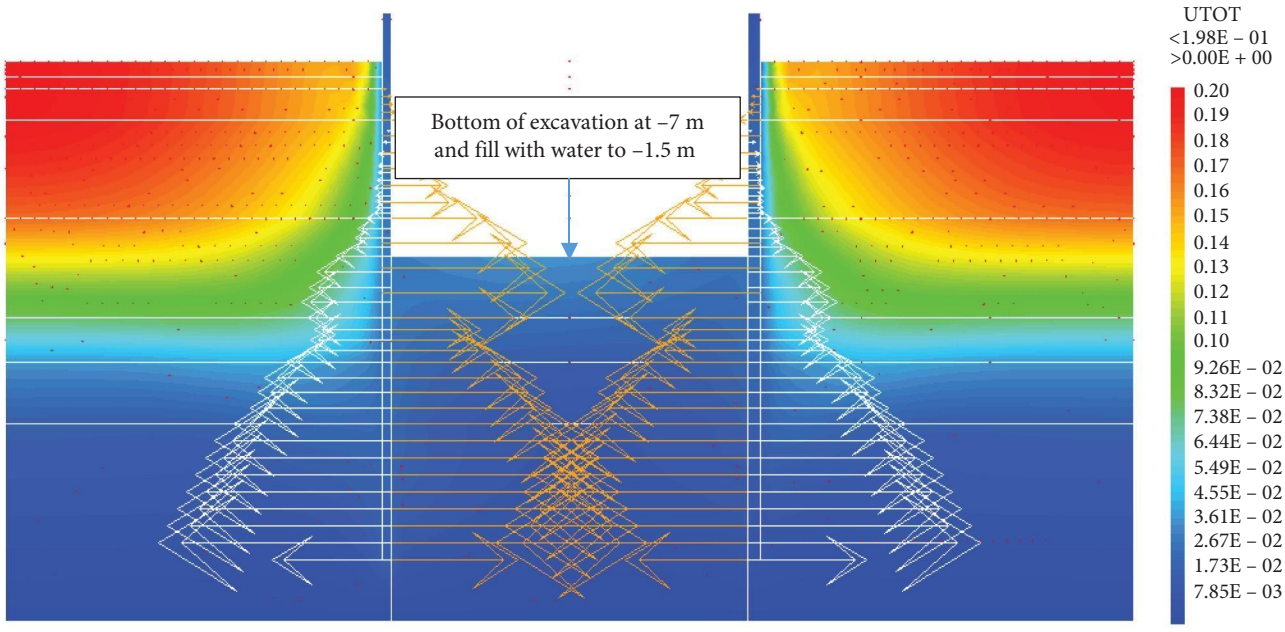

Figure 25: Shadings of the total displacements (m) of the model in phase 5.

phase (Figures 14–16), the variation of the quantities calculated compared to phase 1 remains small. The displacements and plastic strains of the model are almost identical to those of phase 1.

5.4. Phase 3: Excavation Underwater to −7.0 m. This phase is based on the excavation underwater of geostatic stress state in the ground. The excavation of the soft soils between the two walls induces a total displacement of 19 cm out of the excavation and about 1.68 cm inside the excavation. Figures 17–19 present the total displacements and plastic strains (phase 3) of the model. An increase in plastic strains around the walls is observed in Figures 18 and 19. The increase in deviatoric stresses as a function of the depth of the excavation also induces an increase in plastic strains

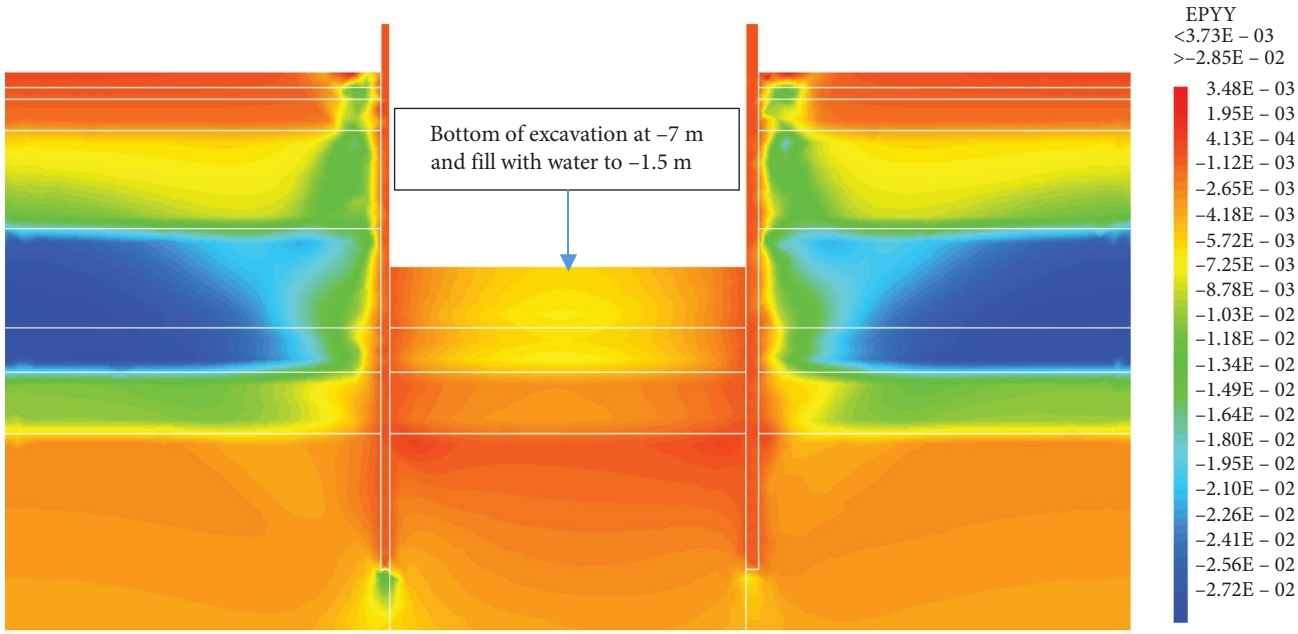

Figure 26: Shadings of the vertical plastic strains of the model in phase 5.

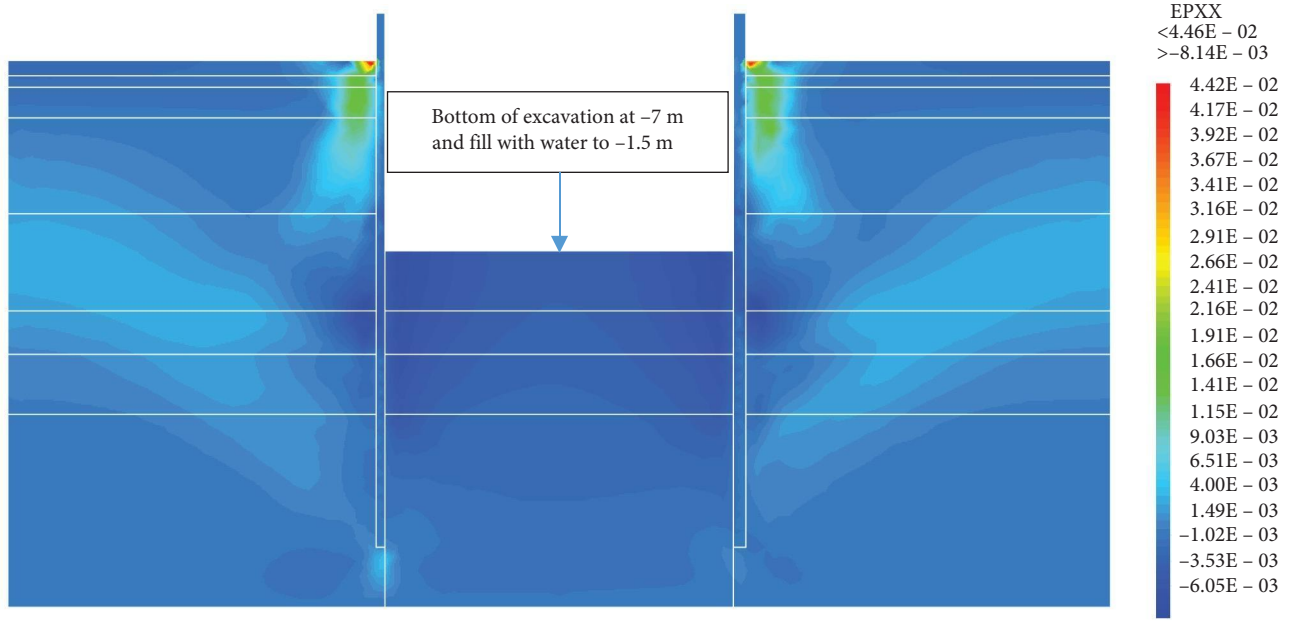

Figure 27: Shadings of the horizontal plastic strains of the model in phase 5.

around the excavated area. Perfect consistency is observed on horizontal displacements within the excavated area on the AZ13 walls (Figure 20). A slight difference is observed on the displacements of the L607K wall. The gap between the numerical and measurement results remains small. The horizontal displacements induced in this phase are significantly higher than those in phase 1.

5.5. Phase 4: Lowering Water Level to −5.0 m. In this phase 4, the lowering water from −1.5 to −5 m is realized. The drop in the water level from −1.5 to −5.0 m causes an increase in plastic stains and horizontal displacements within the excavation. The increase in horizontal displacements on the retaining walls is about three times compared to phase 3 (Figures 21–24). This unconfinement pressure causes strong instabilities around the retaining walls, despite the retention by struts at their tops. The values of plastic strains and lateral displacements on the walls are much higher than those expected for retaining structures (depending on the state-of-the-art).

5.6. Phase 5: Fill with Water to −1.5 m. The fill with water from −5.0 to −1.5 m is observed on the excavation in this

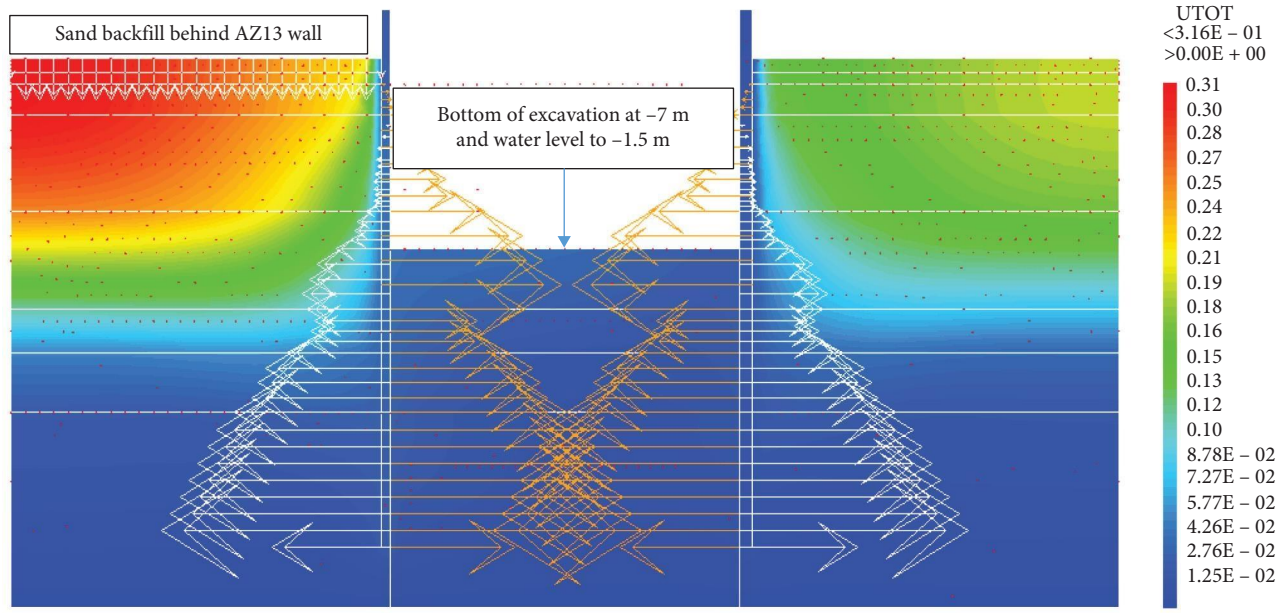

Figure 28: Shadings of the total displacements (m) of the model in phase 6.

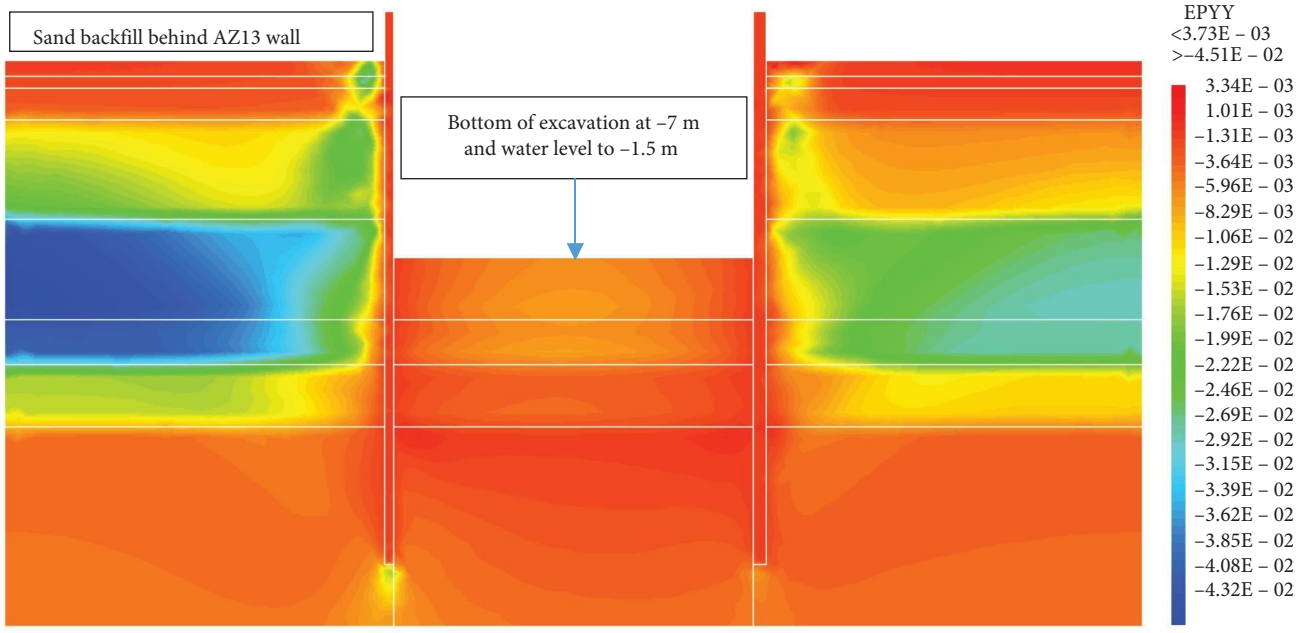

Figure 29: Shadings of the vertical plastic strains in phase 6.

phase 5. The variation of the quantities calculated (Figures 25–27) compared to phase 4 remains small. The displacements and strains of the model are almost identical to those of phase 4. The retaining walls having undergone excessive strains and horizontal displacements in phase 4, the fill with water operation from −5.0 to −1.5 m does not modify the apparent state of stresses in the soft soils.

5.7. Phase 6: Sand Backfill Behind AZ13 Steel Sheet Pile Wall. In this phase 6, the application of surface load for sand backfill behind AZ13 steel sheet pile wall is realized. Figures 28–31 present the total displacements, plastic strains, and horizontal displacements in the walls. The total displacement behind the AZ13 wall reaches 31 cm, it remains of the order of 20 cm behind the L607K wall. This sand backfill creates a great increase in stresses, strains, and displacements around the AZ13 wall. An increase of about 40% in horizontal displacements on the AZ13 wall is observed compared to phase 4 (Figure 31).

5.8. Phase 7: Lowering Water Level to −5.0 m. The lowering water from −1.5 to −5 m is realized. Figures 32–35 present

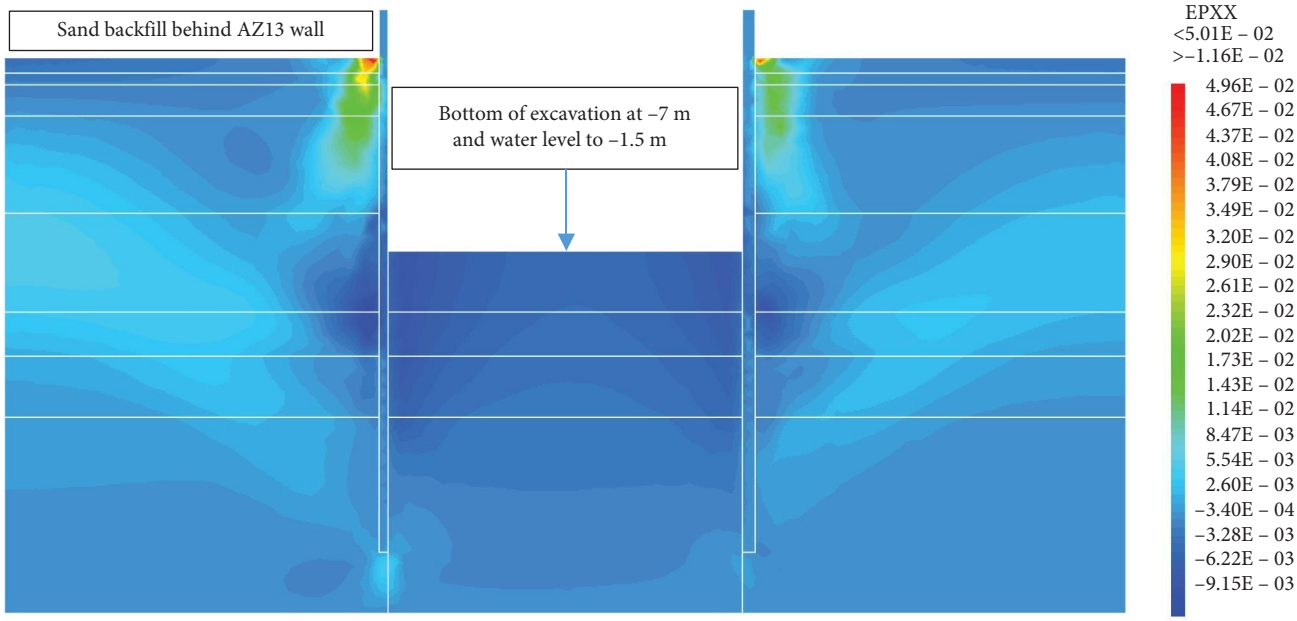

Figure 30: Shadings of the horizontal plastic strains of the model in phase 6.

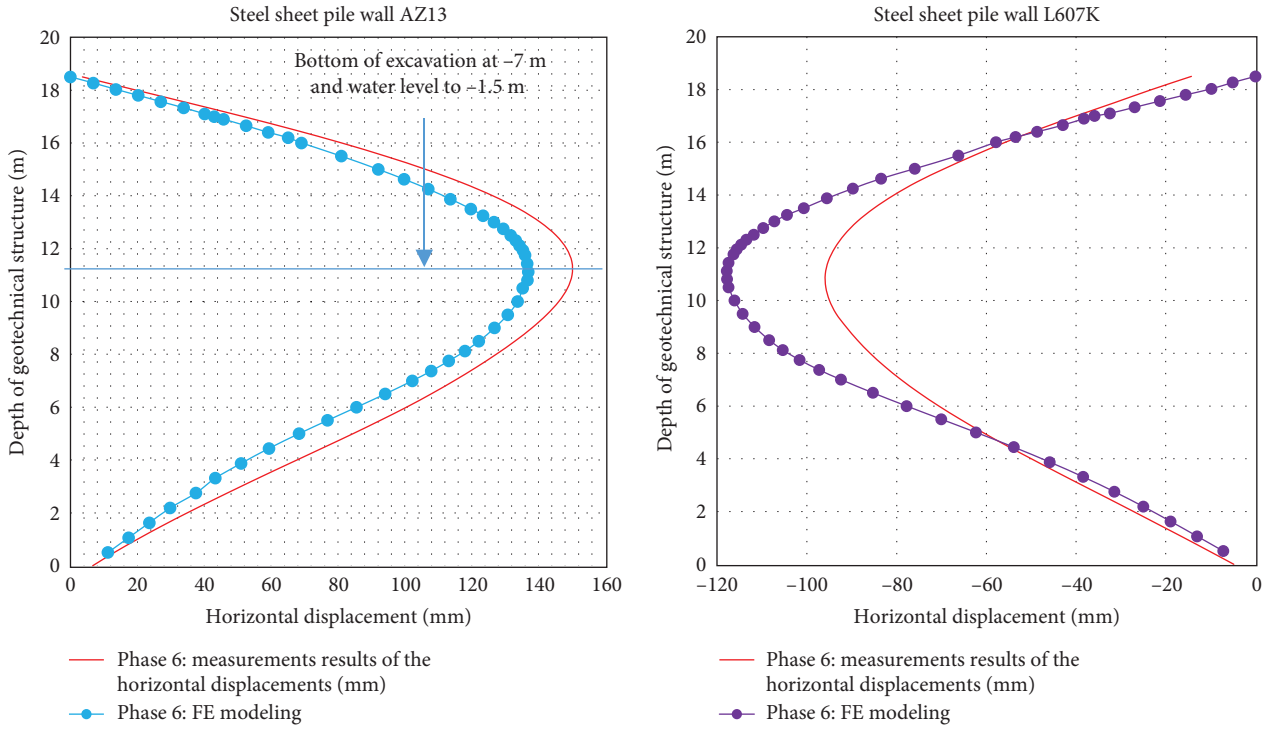

Figure 31: Horizontal displacement in the steel sheet pile walls in phase 6.

the deformed mesh, the total displacements, and plastic strains of the model. The drop in water level from −1.5 to −5.0 m causes an increase in total displacements (33 cm), plastic strains around the AZ13 wall. A slight increase in these sizes is observed around the L607K wall as well.

5.9. Phase 8: Long-Term Performance. The calculation of the long-term behavior of the geotechnical work is performed with progressive drawdown of the water level to the bottom of the excavation (−7.0 m). This drop also causes an increase in total displacements (35 cm), plastic strains, and large horizontal displacements on the retaining walls (Figures 36–39). These lateral movements reach the value of 230×10^{-3} m on the AZ13 wall (against 137 mm in phase 6) and 159 mm for the L607K wall (against 118 mm in phase 6) (Figure 39).

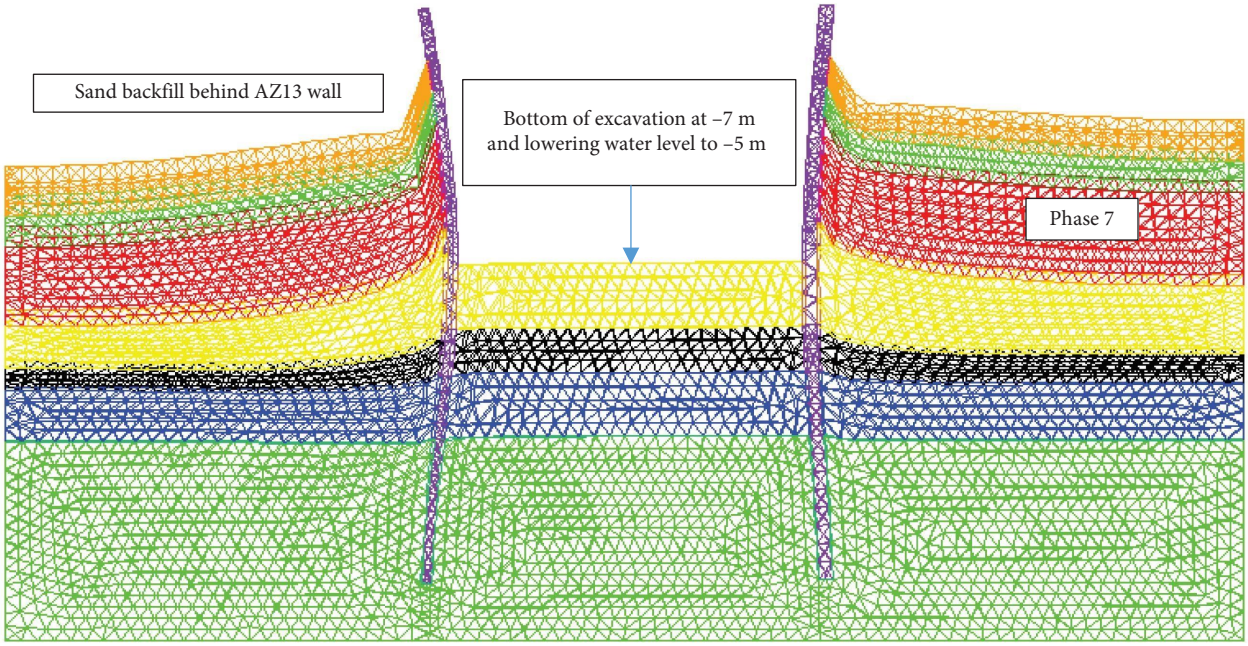

Figure 32: Deformed mesh of the model in phase 7.

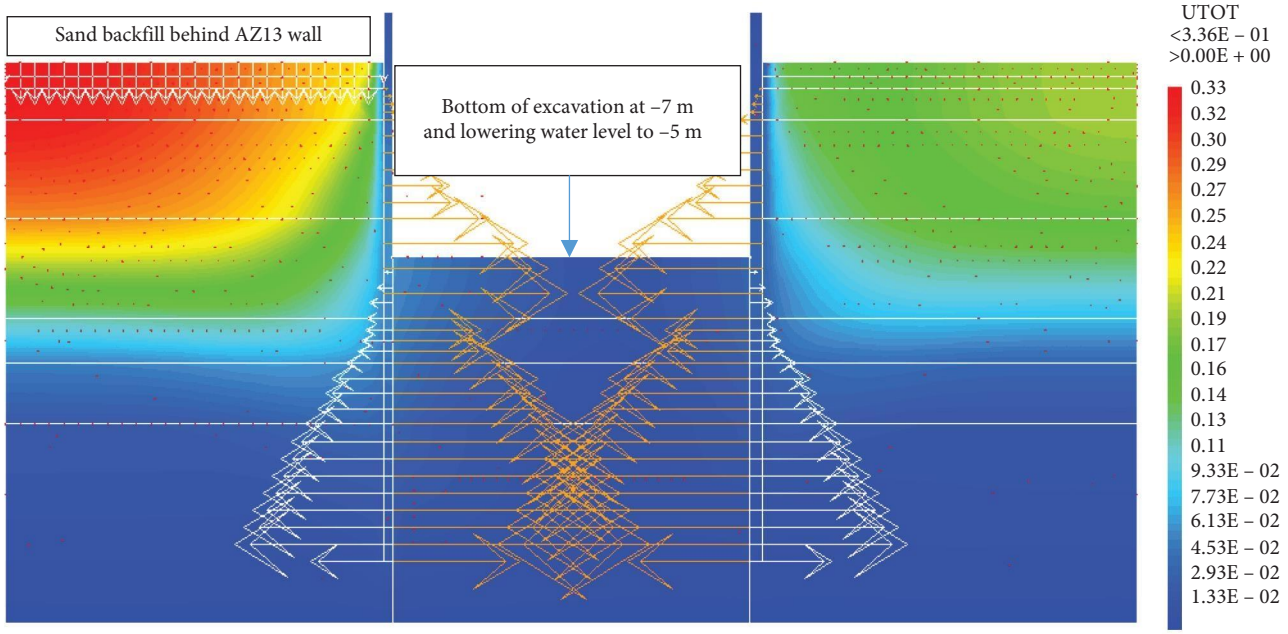

Figure 33: Shadings of the total displacements (m) of the model in phase 7.

6. Discussion

The values of horizontal strains obtained on the steel sheet piles walls greatly exceed those commonly accepted for such structures which are of the order from 10^{-4} to 10^{-3} [40]; hence the need for another struts fixing these large strains. The horizontal deflection curves of the site investigation were determined by means of conventional measures [18]. Measurements and finite element values of the displacements for AZ13 and L607K walls are illustrated in Figures 13, 20, 24, 31, 39, and 40. The results of the horizontal displacements for all phases on the AZ13 and L607K walls are illustrated in Figure 40. For phases 2 and 5 (water rise to −1.5 m), the horizontal displacements were not measured. The differences between the FE calculation and measurement results for the horizontal displacements water pressures and lateral earth pressure are small.

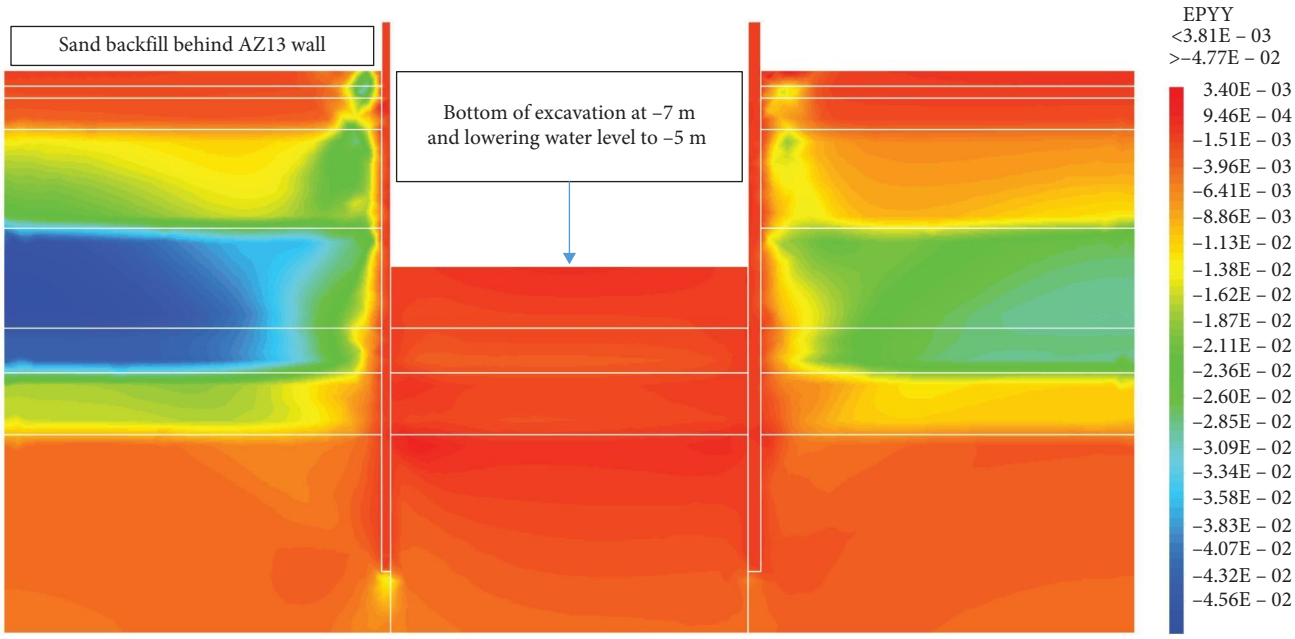

Figure 34: Shadings of the vertical plastic strains in phase 7.

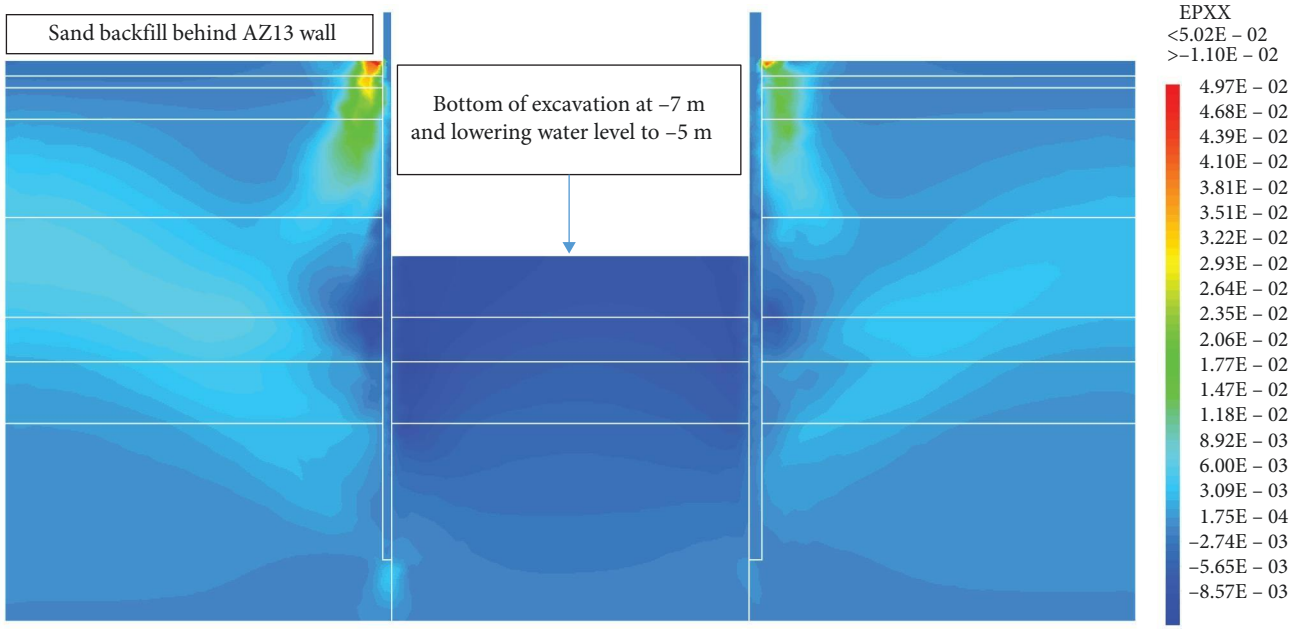

Figure 35: Shadings of the horizontal plastic strains of the model in phase 7.

Vertical and horizontal stresses, including water pressure, increased slightly after the sand backfill was placed. The construction of the embankment behind AZ13 wall caused a significant increase in the pressures on this wall, due to the low rigidity of the soft soils in place. The active thrust condition of the earth was obtained because of this increased pressure, which caused significant horizontal displacements of the AZ13 sheet pile toward the interior of the excavation. The immediate behavior of the construction to refilling of the excavation is observed. The shadings of the vertical plastic strains (Figures 7, 11, 15, 18, 22, 26, 29, 34, and 37) show that excessive plastic strains are localized in the peat layer which has very poor geotechnical characteristics. The largest horizontal plastic strains are located on the top of the soil ground in contact with steel sheet pile walls (Figures 8, 12, 16, 19, 23, 27, 30, 35, and 38). This behavior is justified by the fact that the steel sheet pile walls are blocked at their apex inside the excavation and the first

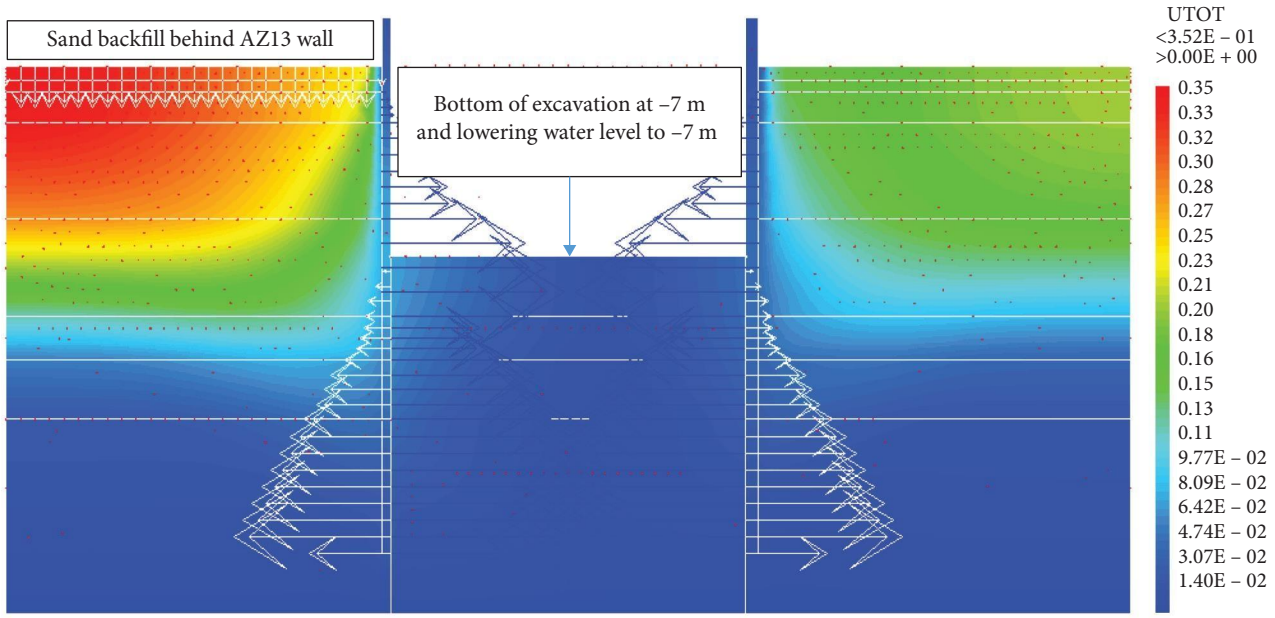

Figure 36: Shadings of the total displacements (m) of the model in phase 8.

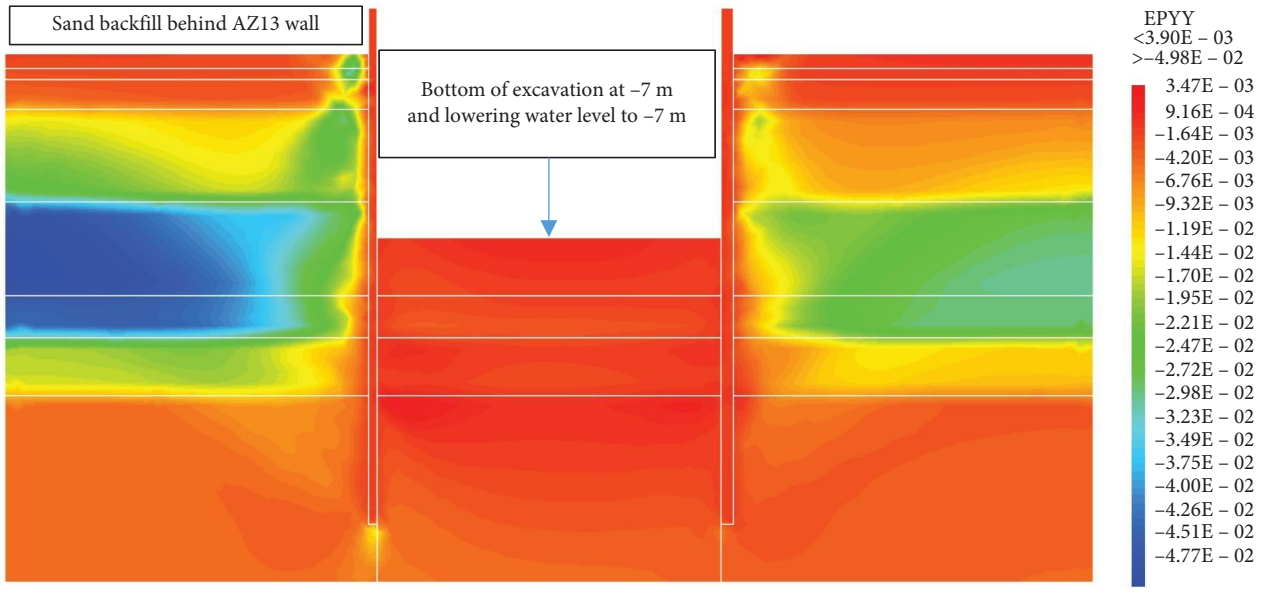

Figure 37: Shadings of the vertical plastic strains in phase 8.

horizontal stresses appear on the first parts in contact with the soil ground. The middle of the so-called steel sheet pile walls becomes flexible depending on the depth of the excavation. The results of on-site measurements through the horizontal displacements curves on the L607K steel sheet pile wall show a loosening of the struts which causes the appearance of horizontal displacements at the apex to the excavated side.

The results of the numerical horizontal displacements through the curves presented show zero movement at the top of the steel sheet pile walls, the correct ones, as they were blocked like the struts on site. These horizontal displacements are located between the top and base of the steel sheet pile walls and increase with the depth of the excavation. For this excavation, it is the gravity unloading which induces the failure of the soil ground by means of an increase in the deviatoric stresses. A rigorous numerical modeling of such a structure is to prevent its failure mechanisms (depending on the stresses and displacements) and to be able to anticipate by taking the necessary solutions to avoid collapses during and after the construction. In the case of deep excavations in submerged soft soils, the maximun horizontal

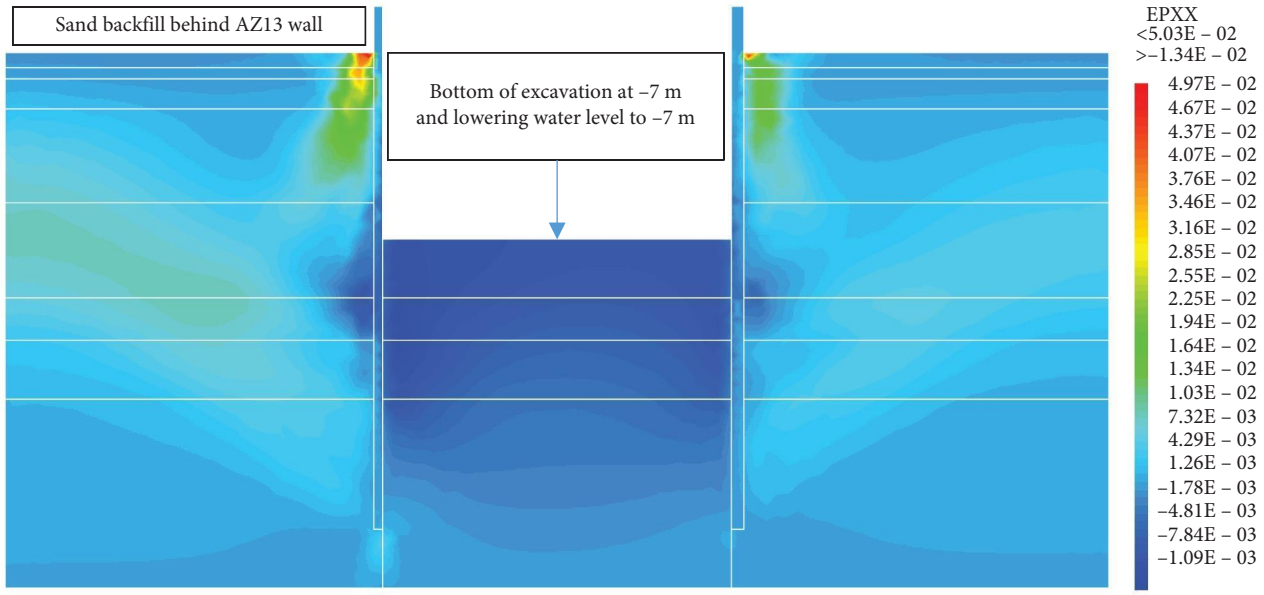

FIGURE 38: Shadings of the horizontal plastic strains of the model in phase 8.

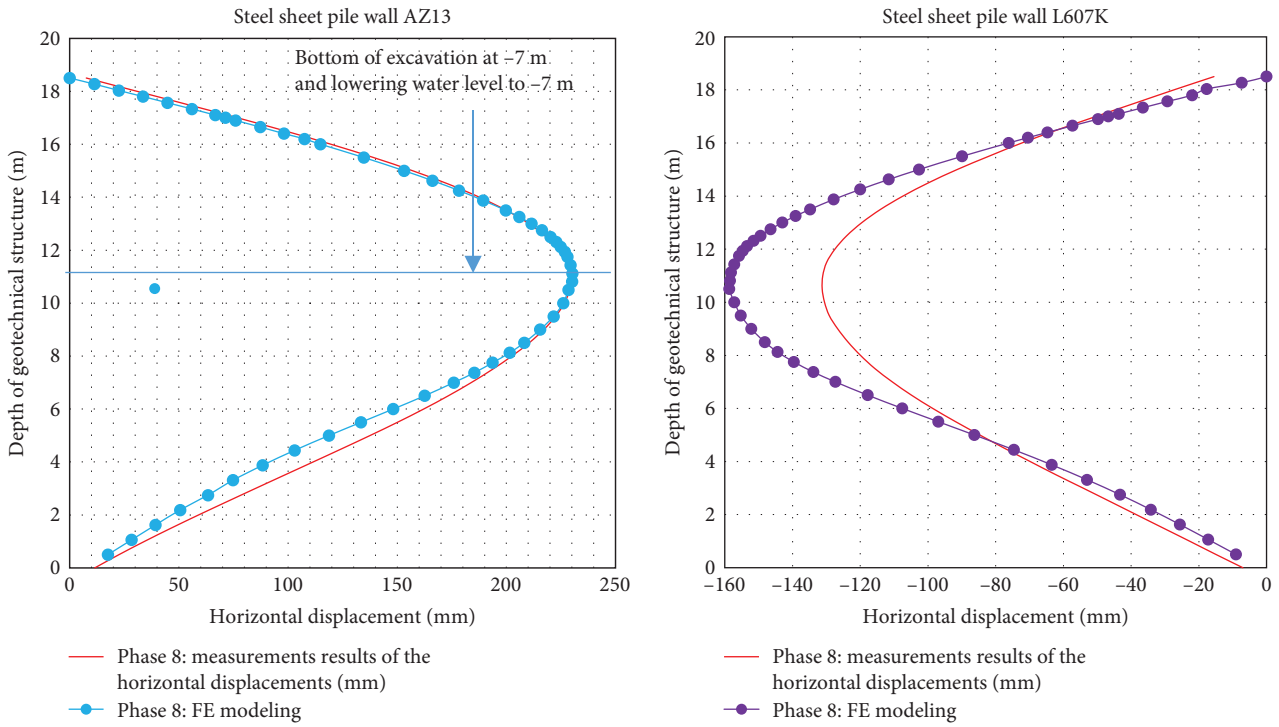

FIGURE 39: Horizontal displacement in the steel sheet pile walls in phase 8.

displacements were set at $u_{max} = 0.02$, $H_0 = 0.14$ m, (H_0: height of excavation) [46]. Observation of the horizontal displacement curves generated by steel sheet pile walls during excavation shows that a second bed (approximately −5.0 m deep) of struts is necessary to prevent these displacements. The transformation of the geometry and stiffness of the steel sheet pile walls to the retaining walls of an equivalent bending stiffness on the one hand and regular geometric shapes allowed in this paper to overcome the difficulties of modeling these steel sheet pile walls in 2D with irregular shapes. The results of this approach are satisfactory in view of the horizontal displacement curves obtained on the steel sheet pile walls compared by the measures.

The Drucker–Prager law used to describe the behavior of the soil models made it possible to realistically predict the response of the geotechnical works following the phases of excavation, lowering or filling the water level in the excavation. This study shows that rigorous modeling (very fine

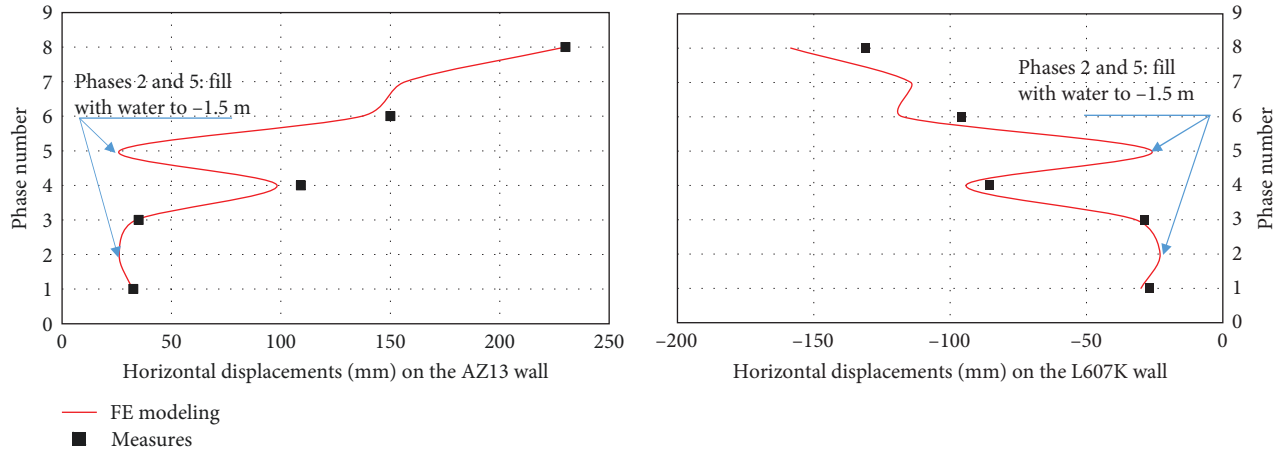

Figure 40: Horizontal displacements in the steel sheet pile walls in phases 1–8.

mesh, behavior laws adapted to the materials, compliance with execution phases) realistically allows the behavior of geotechnical works. The results obtained in this study are of the same order as those resulting from measurements. The designer is able to make decisions that guarantee the durability of his structure according to the functional requirements and the expected lifespan based on rigorous numerical modeling. Such an approach saves large budgets for maintenance and repair operations. Rigorous numerical modeling makes it possible to obtain valid results at reasonable costs without waiting for long delays to draw lessons from full-scale experiments with structures that require very high time and budgets.

7. Conclusion

Cast3M is an FE code dedicated mainly to the calculation of stiff structures. At present, from a methodical, rigorous, and sophisticated computation, we manage to solve complex geotechnical problems both respecting the functional requirements and the different stages of excavation/construction allowing to have the overall stability which guarantees the durability of the geotechnical structure in comfortable safety conditions. The results presented in this paper were compared with those from measurements testifying to the reliability of our rigorous computation from the Cast3M code. Optimization numerical backcalculation results are proposed for retained walls design and construction on the basis of the horizontal displacements, earth and hydraulic pressure measurements. The difficulties of modeling 2D sheet pile walls in 2D with irregular shapes were overcome by transforming the geometry and stiffness of these steel sheet pile walls into retaining walls of equivalent bending stiffness on the one hand and regular geometric shapes on the other hand. The results of this approach are satisfactory in view of the horizontal displacement curves obtained on the steel sheet pile walls compared by the measures. Numerical modeling makes it possible to carry out calculations that contribute to the optimization of geotechnical structures. Nevertheless, if they are poorly carried out, these calculations can lead to erroneous interpretations in the design of geotechnical structures and it is therefore more necessary than ever to know the most important aspects of numerical modeling.

Data Availability

The data used to support the findings of this study are available from the corresponding author upon request.

Conflicts of Interest

The authors confirm that there are no conflicts of interest associated with this publication.

References

[1] D. V. Griffiths and P. A. Lane, "Slope stability analysis by finite elements," *Geotechnique*, vol. 49, no. 3, pp. 387–403, 1999.

[2] D. V. Griffiths, *Stability Analysis of Highly Variable Soils by Elasto-Plastic Finite Elements*, Geomechanics Research Center, Colorado School of Mines, 2000.

[3] D. V. Griffiths, "Stability analysis of highly variable soils by elasto-plastic finite elements," in *Advanced Numerical Applications and Plasticity in Geomechanics*, V. D. Griffiths and G. Gioda, Eds., vol. 426 of *International Centre for Mechanical Sciences*, pp. 159–229, Springer, Vienna, 2001.

[4] Z. Ambassa, J. C. Amba, and N. Tamaskovic, "Implementation of the c-phi reduction procedure in Cast3M code for calculating the stability of retaining walls in the layered backfill with strength parameters reduction by elasto-plastic finite element analysis using field data," *Comptes Rendus Mécanique*, vol. 10, (in press), 2023.

[5] H. B. Bian, X. T. Zhang, and J. F. Shao, "A coupled elastoplastic and visco-plastic damage model for hard clay and its application for the underground gallery excavation," *Underground Space*, vol. 2, pp. 60–72, 2017.

[6] J. T. Blackburn and R. J. Finno, "Three-dimensional responses observed in an internally braced excavation in soft clay," *Journal of Geotechnical and Geoenvironmental Engineering*, vol. 133, no. 11, pp. 1364–1373, 2007.

[7] R. J. Finno and L. S. Bryson, "Response of building adjacent to stiff excavation support system in soft clay," *Journal of Performance of Constructed*, vol. 16, no. 1, pp. 10–20, 2002.

[8] K. Kishida, Y. Cui, T. Iura, M. Nonomura, and M. Kimura, "Discussion on the mechanism of ground improvement method at the excavation of shallow overburden tunnel in difficult ground," *Underground Space*, vol. 1, pp. 94–107, 2016.

[9] S.-M. Liao, S.-F. Wei, and S.-L. Shen, "Structural responses of existing metro stations to adjacent deep excavations in Suzhou, China," *Journal of Performance of Constructed*, vol. 30, no. 4, Article ID 04015089, 2016.

[10] J. Shi, G. Liu, P. Huang, and C. W. W. Ng, "Interaction between a large-scale triangular excavation and adjacent structures in Shanghai soft clay," *Tunnelling and Underground Space Technology*, vol. 50, pp. 282–295, 2015.

[11] Y. Tan and M. Li, "Measured performance of a 26 m deep top-down in excavation in downtown Shanghai," *Canadian Geotechnical Journal*, vol. 48, no. 5, pp. 704–719, 2011.

[12] Y. Tan, X. Li, Z. Kang, J. Liu, and Y. Zhu, "Zoned excavation of an oversized pit close to an existing metro line in stiff clay: case study," *Journal of Performance of Constructed Facilities*, vol. 29, no. 6, Article ID 04014158, 2015.

[13] R. P. Chen, Z. C. Li, Y. M. Chen, C. Y. Ou, Q. Hu, and M. Rao, "Failure investigation at a collapsed deep excavation in very sensitive organic soft clay," *Journal of Performance of Constructed Facilities*, vol. 29, no. 3, 2015.

[14] K. Ishihara, "Collapse of braced excavation in Singapore," in *Proceeding, TC302 Symposium Osaka 2011: International Symposium on Backwards Problem in Geotechnical Engineering and Monitoring of Geo-Construction*, pp. 35–50, Kyoto University, Osaka, Japan, 2011.

[15] G. Zheng, Y. Wang, P. Zhang et al., "Performances and working mechanisms of inclined retaining structures for deep excavations," *Journal of Advances in Civil Engineering*, vol. 2020, Article ID 1740418, 18 pages, 2020.

[16] T. Feng, L. Liu, T. Tong, and M. Zhou, "Numerical study on lateral wall displacement of deep excavation supported by IPS earth retention system," *Underground Space*, vol. 2, no. 4, pp. 259–271, 2017.

[17] Z. Ambassa, J. C. Amba, and J. C. Tchamba, "Modélisation et évaluation de la stabilité d'un talus renforcé par clouage industriel en utilisant la méthode c-phi reduction de Plaxis," *Journal Afrique Science*, vol. 13, no. 1, pp. 381–399, 2017.

[18] D. A. Kort, "*Steel sheet pile walls in soft soil*," PhD thesis, TU Delft, Netherland, Article ID 304, 2002.

[19] P. Nguyen, "*Modélisation numérique des soutènements d'excava-excavation*," PhD thesis, ENPC, Paris, France, Article ID 297, 2003.

[20] A. Lim, C.-Y. Ou, and P.-G. Hsieh, "A novel strut-free retaining wall system for deep excavation in soft clay: numerical study," *Acta Geotechnica*, vol. 15, no. 6, pp. 1557–1576, 2020.

[21] A. Gholampour and A. Johari, "Reliability-based analysis of braced excavation in unsaturated soils considering conditional spatial variability," *Computers and Geotechnics*, vol. 115, no. 3, Article ID 103163, 2019.

[22] M. Huang and C.-Q. Jia, "Strength reduction FEM in stability analysis of soil slopes subjected to transient unsaturated seepage," *Computers and Geotechnics*, vol. 36, no. 1-2, pp. 93–101, 2009.

[23] T. P. Huy, Z. O. Htet, and J. Cheng, "Stability of slope and seepage analysis in earth dam using numerical finite element model," *Study of Civil Engineering and Architecture (SCEA)*, vol. 2, no. 4, pp. 104–108, 2013.

[24] Y. Yang, F. Liu, and W. Wu, "Assessing slope stability with an improved 3D numerical manifold method," *Rock Mechanics and Rock Engineering Journal*, vol. 55, no. 10, pp. 6409–6423, 2022.

[25] F. S. Wong, "Uncertainties in FE modeling of slope stability," *Computers & Structures*, vol. 19, no. 5-6, pp. 777–791, 1984.

[26] S. W. Sloan, "Geotechnical stability analysis," *Geotechnique*, vol. 63, no. 7, pp. 531–571, 2013.

[27] F. Tschuchnigg, H. F. Schweiger, S. W. Sloan, A. V. Lyamin, and I. Raissakis, "Comparison of finite-element limit analysis and strength reduction techniques," *Geotechnique*, vol. 65, no. 4, pp. 249–257, 2015.

[28] A. Johari and A. R. Kalantari, "System reliability analysis of soldier-piled excavation in unsaturated soil by combining random finite element and sequential compounding methods," *Bulletin of Engineering Geology and the Environment*, vol. 79, no. 6, pp. 2777–2798, 2020.

[29] A. Johari and Y. Peiro, "Determination of stochastic shear strength parameters of a real landslide by back analysis," *International Journal of Reliability, Risk Safety: Theory and Application*, vol. 4, no. 1, pp. 7–16, 2021.

[30] S. Bozkurt, A. Abed, and M. Karstunen, "Finite element analysis for a deep excavation in soft clay supported by lime-cement columns," *Computers and Geotechnics*, vol. 162, Article ID 105687, 2023.

[31] P. Mestat, "Lois de comportement des géomatériaux et modélisation par la méthode des éléments finis," in *Etudes et recherches des Laboratoires des Ponts et Chaussées-série géotechnique (GT 52)*, 1993.

[32] A. J. Abbo and S. W. Sloan, "A smooth hyperbolic approximation to the Mohr–Coulomb yield criterion," *Computers & Structures*, vol. 54, no. 3, pp. 427–441, 1995.

[33] Z. Ambassa and J. C. Amba, "Assessment of stiffness and strength parameters for the soft soil model of clays of Cameroon," *International Journal Advances in Civil Engineering*, vol. 2020, Article ID 8877367, 16 pages, 2020.

[34] Z. Ambassa, J. C. Amba, and F. X. Mbelen, "Monitoring and numerical modeling of the full-scale experimental embankment on soft Douala clays of Cameroon," *International Journal of Civil Engineering and Technology*, vol. 11, no. 7, pp. 1–9, 2020.

[35] P. Mestat and P. Humbert, "Référentiel de tests pour la vérification de la programmation des lois de comportement dans les logiciels d'éléments finis," *Bulletin des laboratoires des ponts et chaussées*, vol. 230, pp. 23–38, 2001.

[36] P. Mestat, "Validation du progiciel CESAR-LCPC en comportement mécanique non linéaire," vol. 1, Fondations superficielles et tunnels, Rapport d'études et de recherches, Article ID 179, 1994.

[37] Z. Ambassa and J. C. Amba, "Towards an advanced new emerging method of determination of Mohr–Coulomb parameters of soils from at the oedometric test: case study-lateritic soils of Cameroon," *Mathematical Problem in Engineering*, vol. 2022, Article ID 4222654, 18 pages, 2022.

[38] Cast3M©, "Cast3M is a research FEM environment; its development is sponsored by the French Atomic Energy Commission," 2022.

[39] O. C. Zienkiewicz, S. Valliappan, and I. P. King, "Elasto-plastic solution of engineering problems, initial stress, finite element approach," *International Journal for Numerical Methods in Engineering*, vol. 1, no. 1, pp. 75–100, 1969.

[40] O. Zienkiewicz, R. L. Taylor, and J. Z. Zhu, *The Finite Element Method: Its Basis and Fundamentals*, Elsevier, 7th edition, 2005.

[41] D. M. Potts and L. Zdravkovic, *Finite Element Analysis in Geotechnical Engineering: Theory*, Thomas Telford, London, Article ID 444, 2001.
[42] D. M. Potts and L. Zdravkovic, "Accounting for partial material factors in numerical analysis," *Geotechnique*, vol. 62, no. 12, pp. 1053–1065, 2012.
[43] D. C. Drucker, "A more fundamental approach to plastic stress-strain analysis," in *Proceedings of the First UN International Congress for Applied Mechanics*, pp. 487–491, 1951.
[44] N. Tamaskovics, "Stability calculation with FEM with strength parameter reduction," *Geotechnik*, vol. 42, no. 2, pp. 88–97, 2019.
[45] F. Taiyari, M. Kharghani, and M. Hajihassani, "Optimal design of pile wall retaining system during deep excavation using swarm intelligence technique," *Journal of Structures*, vol. 28, pp. 1991–1999, 2020.
[46] R. B. Peck, "Deep excavations and tunnelling in soft ground," in *Proceedings of the 7th International Conference on Soils Mechanics and Foundation Engineering, Mexico*, pp. 225–290, 1969.